Natural Hazards
https://doi.org/10.1007/s11069-024-06615-z

ORIGINAL PAPER

Investigating the impact of tropical deforestation on Indian monsoon hydro-climate: a novel study using a regional climate model

Abhishek Lodh[1,2,3] · **Stuti Haldar**[4,5]

Received: 17 August 2023 / Accepted: 2 April 2024

Abstract
This study uses a state-of-the-art regional climate model (RCM) to examine how tropical deforestation affects the meteorology of the Indian Summer Monsoon (ISM). Incorporating insights from existing research on deforestation by climate scientists, alongside evidence of environmental deterioration in semi-arid, hilly and tropical regions of Southeast Asia, this research seeks to elucidate the critical influence of anthropogenic reasons of climate change on the hydroclimate of ISM. Employing "tropical deforestation" design experiments with the ICTP-RegCMv4.4.5.10 RCM the study evaluates the effects on meteorological parameters including precipitation, circulation patterns and surface parameters. This experimental design entails substituting vegetation type in the land use map of RegCMv4.4.5.10 model, such as deciduous and evergreen trees in Southeast Asia with "short grass" to mimic tropical deforestation. Findings reveal that deforestation induces abnormal anti-cyclonic circulation over eastern India curtails moisture advection, diminishing latent heat flux and moisture transport, leads to a decrease in precipitation compared to control experiment scenario. Alterations in albedo and vegetation roughness length attributable to deforestation impact temperature, humidity, precipitation, consequently exacerbating drought and heatwave occurrences. Additionally, the study also explores deforestation-induced feedback on ISM precipitation variability. The study concludes that deforestation substantially alters land-surface characteristics, water and energy cycle, and atmospheric circulation, thereby influencing regional climate dynamics. These findings offer foundational insights into comprehending land-use and land-cover changes and their implications for climate change adaptation strategies.

Keywords Regional climate modelling · RegCMv4.4.5.10 · Tropical deforestation · Albedo change · UW-PBL · Holtslag-PBL · Precipitation response · Droughts · Climate mitigation

1 Introduction

Anthropogenic activities such as tropical deforestation are eroding carbon sinks and driving the release of greenhouse gasses (GHG) to the atmosphere (Watson et al. 1997; Stocker et al. 2013). These emissions alter the regional and global climate patterns and can impact

Extended author information available on the last page of the article

the ability to predict and react to important weather events. Indian summer monsoon (ISM) is the seasonal migration of winds from equatorial region towards the Indian monsoon zone with changes in the atmospheric circulation features in lower and upper atmosphere. In the twenty-first century climate change scenario, the ISM activity over the Indian subcontinent is known to be linked to both atmospheric GHG content and the alterations of vegetative cover associated with intensive forest management. The ability to predict the conditions of monsoon events is important because in addition to climate impacts, it also has significant socio-economic implications. Studies using remote sensing across the tropics have revealed that during the 1990s and the 2000s, net deforestation increased by 62 percent (Kim et al. 2015). Due to its connection to major weather patterns, deforestation poses acute threats to human health, ecological systems and other socio-economic sectors (Revi et al. 2022). Thus, it is crucial to understand the impact of increasing deforestation rates on monsoon variability to estimate, adapt and mitigate its wide-ranging socio-economic ramifications. This is especially true in resource-constrained underdeveloped and developing economies such as in India. Agriculture is a key sector susceptible to the repercussions of tropical deforestation and other land degradation activities. Recently, leaders from across the globe met at the 27th annual United Nations Climate Change Conference (COP27) held in Sharm El-Sheikh, Egypt, resulting in the commitment to halt and reverse deforestation and land degradation by 2030. India in particular risks falling short of its commitments to combat climate change if urgent action is not taken. Deforestation extends beyond a simple, local ecological concern by exerting controls on large-scale monsoon patterns that are detrimental to human health and agricultural supply chains (Yasuoka and Levins 2007; Lawrence and Vendecar 2015). These manifestations of climate variability either due to natural or man-made reasons, presents substantial financial implications, as they mandate considerable expenditure for adaptation and policy adjustments regarding resource utilization, diverting public investments away from key sectors such as education, health and other basic services (Chambwera et al. 2014; Farid et al. 2016; Srinivasan et al. 2023). Thus, the forested areas of the Indian subcontinent hold economically important natural resources such as coal and iron-ore. Extraction of these essential minerals not only leads to deforestation, but also reduces the capacity of the region to act as carbon sinks. Therefore, the magnitude of tropical deforestation has significant environmental and sociological implications (Strandberg et al. 2023). Notably, deforestation leads to desertification which further compounds environmental challenges by reducing the recovery capacity of formerly forested land area. Desertification refers to the deterioration of land in regions with arid, semi-arid, and dry sub-humid climates, driven either by natural climate change and/or human action (Lodh 2021). For example, deforestation can result from urban expansion and industrial growth such as agricultural land conversion. In the tropics, both desertification and deforestation have been responsible for shifts in local and regional weather and climate (e.g. in the Thar desert, India and deforestation in north-east India). As per the Food and Agriculture Organization of the United Nations (FAO), deforestation entails changing forest areas to other types of land uses such as farming lands, urbanized zones, barren lands, or any other usage that leads to a significant decrease in tree canopy, dropping below a 10% threshold (Lodh 2021). Hence, halting deforestation is crucial for efforts to limit global warming to less than 1.5° Celsius and reduce the rate of biodiversity loss and protect jobs and livelihoods. Forests can act as both source and sinks of carbon dioxide. Forests worldwide release approximately 8.1 billion metric tons of carbon dioxide annually as a result of deforestation and other land-related disruptions, whereas they intake about 16 billion metric tons of carbon dioxide each year (Harris et al. 2021).

Studying the land surface mechanisms in the dry and semi-dry areas of north-west India, reveals their impact on mesoscale atmospheric circulations at a regional scale (Bollasina and Nigam 2011; Lodh 2020; 2021). This can occur through the transfer of heat, moisture and momentum between the Earth's surface and the atmosphere (BaidyaRoy and Avissar 2002). Previous studies using general circulation models have indicated that global climate change resulting from land-use and land-cover changes, particularly deforestation and land degradation, has severe consequences on weather and climate (Henderson-Sellers et. al. 1993; Xue and Shukla 1993; Polcher and Laval 1994a, b; Gupta et al. 2005; Hasler et al. 2009). The land surface and its vegetation interact directly with the atmosphere to exchange heat and moisture. Consequently, they play a pivotal role in moderating responses within the climate system (Polcher and Laval 1994b; Pielke et al. 1998). Significant reduction in precipitation over Indian land region (~18%) has been reported due to impacts of deforestation across monsoon impacted regions, due to shift in Inter-Tropical convergence zone (Devaraju et al. 2015). Similar studies project that, rapid deforestation over India would result in a decrease in rainfall over north India by 2 mm/day (Gupta et al. 2005). Polcher and Laval 1994b modeled the impacts of deforestation to be statistically significant and independent of ENSO effects. Bathiany et al. (2010) reported that complete deforestation of the tropics would exert a global warming of 0.4 degree Celsius. Spracklen and Garcia-Carreras (2015) asserted that by the 2050s deforestation will reduce regional rainfall over the Amazon basin by 12% (21%) in the wet (dry) season. Under global climate warming, there are increasing uncertainties on the projections of compounded extreme weather events, leading to low confidence of how their impacts will feedback into future climate change. Thus, improved sensitivity and accuracy of numerical models tuned to currently observed land use change (like tropical deforestation scenarios) are important for better predicting the impacts of future global change.

Pioneering climate modeling work on deforestation induced shifts in land-surface albedo (Charney 1975; Charney et al. 1975, 1977; Dickinson et al. 1983) forms the motivation for the tropical deforestation design simulations conducted in this study. Although there have been prior attempts to understand the biogeophysical aspects of tropical deforestation, the central aim of this research is to investigate tropical deforestation within the scope of the Biosphere–Atmosphere Transfer Scheme (BATS) vegetation module coupled with RegCMv4.4.5.10 model, over southeast Asia. This is achieved by conducting climate model experiments involving changes in vegetation i.e. a proxy for land use land cover (LULC) change design experiments. The objective is to derive findings that not only support, but also enhance the insights obtained from earlier research endeavors (Xue and Shukla 1993; Polcher and Laval 1994a, b; Werth and Avissar 2002, 2005a, b; Gupta et al. 2005; Bollasina and Nigam 2011; Devaraju et al. 2015; Spracklen and Garcia-Carreras 2015) while delving into the question of whether the degradation of land and the deforestation of tropical regions exert significant influences on the meteorological patterns of the Indian monsoon.

The idea is to identify potential alterations in regional precipitation and circulation trends within the Indian monsoon system by means of carefully devised sensitivity experiments. These experiments seek to elucidate the underlying mechanisms that govern the interplay between land surface and vegetation, with a specific focus on the impacts of land degradation and tropical deforestation. Hence, to investigate feedback due to anthropogenically changing biogeophysical scenarios to the atmospheric circulations over the Indian subcontinent, the study conducted in this paper is important for identifying and bridging the gap in extant literature. In the wake of the recent COP 27 summit in Egypt, there is global consensus recognizing the urgent need for effective adaptation and mitigation

strategies against climate change. Hence, the study conducted in this paper aligns with this broader discourse by estimating the risks of climate variability on land and ecosystems and their ripple effects in economic and social systems. In countries such as India, where there's a limited capacity for adaptation and mitigation, the consequences of climate variability are particularly evident (Rasul and Sharma 2016). Tropical monsoons are vital for irrigation in these countries, and any disruption can threaten the agriculture that millions depend on for their livelihoods and food security (Marambe et al. 2015). Unfavorable changes in the monsoon patterns, thus, bear heavily on the poor and the vulnerable communities in the rural areas which further triggers forced migration (Clement et al. 2021). Moreover, deforestation disrupts local and regional climate patterns that results in unpredictable temperature variability, humidity fluctuations, and heat stress that potentially leads to fatalities (Kovats and Hajat 2008). In economic terms, the crowding out of investments from critical sectors like education, health care, infrastructure, and energy are some of the indirect risks associated with the financial burden of climate change adaptation and mitigation (Chambwera et al. 2014). Whereas, at the macro level, reduced agricultural productivity directly translates to falling export revenues and increased reliance on food imports, further constricting the state's fiscal capacity.

Thus, understanding the intricate relationships between deforestation, monsoon variability, and their socioeconomic implications is crucial for devising effective adaptation strategies. This calls for an evidence-based policy making and governance that prioritizes sustainable land use planning, afforestation, and reforestation efforts to curtail the climate induced risks (Pörtner et al. 2022). The findings of this paper are relevant not only for India but also other Low- and Middle-Income Countries (LMICs) with populations substantially dependent on land and ecosystem services for their livelihoods. The framework of this study is underpinned by the IPCC AR6's emphasis on socially just and equitable climate resilient development pathways (New et al. 2022). Therefore, the study aims to serve as a catalyst for informed, impactful policymaking, thereby fostering a sustainable future.

2 Materials and methods

2.1 Brief model description and region of study

The model used in this study is RegCM (version 4.4.5.10) which is one of the first limited area community model from ICTP (Dickinson et al. 1989). Operating on an Arakawa B-grid, RegCM is a hydrostatic, compressible model that utilizes a sigma-p vertical coordinate system. In this model, thermodynamic and wind variables are staggered horizontally, employing a time-splitting explicit integration approach. The model dynamics are resolved using horizontal momentum, continuity and thermodynamic equations. The calibrated version 4.4.5.10 of the ICTP regional climate model (RCM), RegCMv4.4.5.10, has the capability to simulate a range of atmospheric and land surface processes, including radiation, precipitation, soil moisture and vegetation dynamics, at high spatial and temporal resolutions. The RegCMv4.4.5.10 was installed in "parallel" mode at the central high-performance computing facility of the Indian Institute of Technology, Delhi. The model domain is over South Asia, spanning 17°E—123°E and 16°S—40°N, with a horizontal resolution of 60 km and 18 vertical levels in the atmosphere (using sigma coordinate) as shown in Fig. 1a. Different RCM studies have meritoriously used the ICTP-RegCM model for its

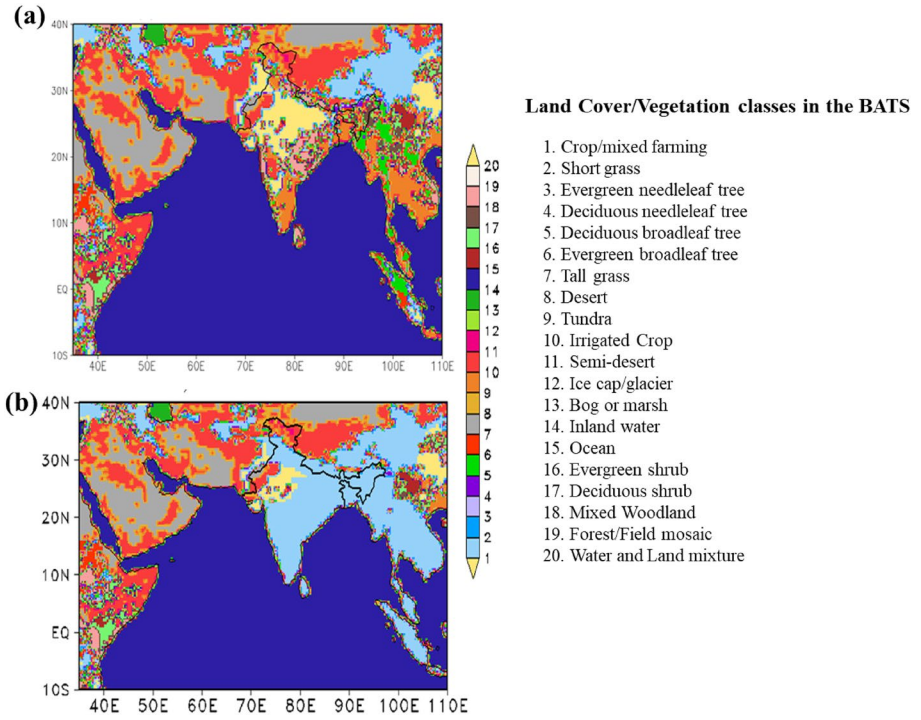

Fig. 1 **a** Control landuse map in the baseline experiment (**b**) modified land use map for the deforestation experiment using BATS coupled RegCMv4.4.510 model (*the legend colors represent the land cover/ vegetation classes in the BATS land surface model)

research purpose (Giorgi et al. 2012, 2015; Dash et al. 2015; Lodh 2017; 2021; Camara et al. 2022).

2.2 Details of the control experiment

The RegCMv4.4.5.10 model is a regional climate model that accurately simulates atmospheric, cloud microphysics, land surface, planetary boundary layer and radiation processes. In this study, the BATS coupled RegCMv4.4.5.10 model (Dickinson et al. 1993; Elguindi et al. 2014) is invoked for numerical simulations (for both Control and tropical deforestation design experiments). The BATS1E vegetation scheme incorporates twenty vegetation types, soil textures ranging from fine (clay) to intermediate (loam), to coarse (sand) and different soil colors (light to dark) for the soil albedo calculations (Dickinson et al. 1986). The BATS scheme comprises of a vegetation layer, a layer for snow, a surface soil layer with a thickness of 10 cm, a root zone layer spanning 1–2 m and a third layer of deep soil measuring 3 m in thickness. The latent heat (LHF) and sensible heat (SHF) formulations are calculated from the bulk aerodynamic formulations. For the control run, the Emanuel convection scheme over land and the Grell convection scheme over the ocean, is combined with the Arakawa Schubert 1974 closure, along with the University of Washington planetary boundary layer (PBL) and Holtslag scheme, for the two sets of control experiments. They are abbreviated as RCM-CONTROL-UW and RCM-CONTROL-Holtslag,

respectively. In RCMs, PBL parameterization is employed to depict the impacts of subgrid-scale turbulence that cannot be explicitly resolved due to the model grid's limited resolution. Parametrizing the boundary layer in climate models is essential for replicating processes within the boundary layer, such as vertical mixing and other turbulence-related phenomena. The UW turbulence closure scheme (Bretherton et al. 2004) is a 1.5-order local, down-gradient diffusion parametrization scheme possessing the capability to compute vertical fluxes within and outside of the PBL. The UW scheme also integrates directly the emission and deposition flux terms as part of the calculation of turbulent tracer tendency. The Holtslag PBL scheme (Holtslag et al. 1990; Holtslag and Boville 1993) adopts a non-local diffusion concept, considering counter-gradient fluxes arising from large-scale eddies in an unstable mixed atmosphere. For more detailed information, please refer to Elguindi et al. (2014). The details and results of the second control simulation, RCM-CONTROL-HOLTSLAG (Emanuel over land and Grell over ocean with Arakawa Schubert 1974 closure and Holtslag PBL scheme) are described in detail in Lodh (2021). The lateral boundary condition scheme employed is relaxation, exponential technique. The Subgrid Explicit Moisture Scheme (SUBEX) resolves the non-convective clouds and precipitation by linking the average grid cell humidity to the cloud fraction and cloud water (Elguindi et al. 2014; Sundqvist et al. 1989). The auto-conversion rate over land and ocean is 0.250E-03. The details of the control experiments (RCM-CONTROL-UW and RCM-CONTROL-HOLTSLAG) are provided in Table 1.

2.3 LULC map

The contemporary state of land cover mapped data over India as represented by the Global Land Cover Characterization (GLCC) datasets, used in the control simulations are shown in Fig. 1a. Figure 1b shows the LULC change map as used in the deforestation design experiment. "Tropical deforestation" is mimicked in the RCM by replacing vegetation classes along the principal axis of Asian monsoon i.e. over the tropical rain-belt regions over Myanmar, Indonesia, Sumatra, Thailand and Cambodia (Indo-Chinese peninsula, and Maritime subcontinent) by short grass. Terrestrial variables like elevation, sea surface temperature, and three-dimensional isobaric meteorological data are horizontally interpolated from a latitude–longitude mesh to a high-resolution ($166 \times 108 \times 18$) domain on either a Rotated Mercator (ROTMER) projection.

2.4 Details of the deforestation design experiment

In the context of the deforestation design experiment, specific regions within north-east India, Eastern Ghats, Western Ghats, Indo-Gangetic plains, peninsular India and areas along the principal axis of the monsoon (encompassing Myanmar, Indonesia, Sumatra, Thailand, and Cambodia) are designated for alteration in LULC to mimic tropical deforestation in the model. These regions, originally in the LULC map is classified as having "forest" vegetation, irrigated crops and mixed farming are replaced with "short grass" in the RCM. This modification is applied to the original ASCII test land use map utilized for the RCM's control simulation. The primary objective here is to isolate and analyze the climate change signal arising from tropical deforestation. The conversion process involves changing the land cover to "short grass" in all regions along the path of the monsoon's principal axis where tropical deforestation is implemented. This shift to "short grass cover" aligns with findings from various studies (Scharn et al. 2021) indicating an increase in the

Table 1 List of deforestation design experiments using Regional climate model, RegCMv4.4.5.10

Experiment name	Model details: domain, grid spacing and region of prescribed vegetation change	Land-surface condition and duration of simulation run	Details of parameterization schemes used
1. RegCM4.4.5.10-CONTROL-1 (REGCM445-1) [abbreviated as RCM-CONTROL-UW] 2. RegCM4.4.5.10-CONTROL-2 (REGCM445-2) [abbreviated as RCM-CONTROL-HOLTSLAG]	17°E-123°E, 16°S- 40°N, (166 × 108 × 18); ~60 km resolution; GLCC LULC Model Timestep: 30 s Central latitude and longitude of model domain is 16°N and 70°E Model top pressure: 5 cbar	Land use category as defined in BATS1E Global Land Cover Characterization datasets from USGS are used to create vegetation and land use data files. (http://users.ictp.it/~pubregcm/RegCM4/globedat.htm#part5) 00UTC of 1st October 1999 to 00UTC of 1st January 2011 (simulation length is 98,640 h)	(a) Emanuel over land and Grell over ocean with Arakawa Schubert (AS) 1974 closure and UW PBL scheme (c) Emanuel over land and Grell over ocean with Arakawa Schubert (AS) 1974 closure and Holtslag PBL scheme. *(Lodh A. 2020, Theoretical and Applied Climatology)*
3. RegCM4.4.5.10- DEFORESTATION -1 [abbreviated as RCM-DEF-UW] 4. RegCM4.4.5.10- DEFORESTATION-2 [abbreviated as RCM-DEF-HOLTSLAG]	17°E-123°E, 16°S- 40°N, (166 × 108 × 18); ~60 km resolution Modified extended desert LULC Model Timestep: 30 s Central latitude and longitude of model domain is 16°N and 70°E Model top pressure: 5 cbar	Deforestation is done over India and regions covered by the principal axis of monsoon (i.e. over Indo-China peninsula and maritime subcontinent) (See Fig. 1b) 00UTC of 1st October 1999 to 00UTC of 1st January 2011 (simulation length is 98,640 h)	(a) Emanuel over land and Grell over ocean with Arakawa Schubert (AS) 1974closure and UW PBL scheme (b) Emanuel over land and Grell over ocean with Arakawa Schubert (AS) 1974 closure and Holtslag PBL scheme

prevalence of evergreen shrubs. This phenomenon is driven by soil moisture conditions, which are in turn influenced by precipitation patterns.

Similar to the control experiments, the convection scheme is Emanuel over land and the Grell scheme over the ocean, combined with the Arakawa Schubert 1974 closure. For the tropical deforestation design experiments titled RegCMv4.4.5.10—DEFORESTATION, both the University of Washington and Holtslag PBL schemes are utilized. They are abbreviated as RCM-DEF-UW and RCM-DEF-Holtslag, respectively. Since the sensitivity to LULC change is dependent on the choice of parametrization and RCM used, hence we use two different PBL schemes. In these experiments, the original ASCII text land use map from the control simulation is modified to incorporate the land use change for the tropical deforestation design experiments. Important BATS vegetation parameters relevant to the tropical deforestation design experiments, such as roughness length, vegetation albedo, maximum fractional vegetation cover, and leaf area index, for the land use type "short grass" are provided in Table 2. In the Holtslag PBL scheme, the value of critical Richardson number for land and ocean is 0.25. In the UW PBL scheme, standard T-Q_V-Q_C advection is employed with 15 as the efficiency value of enhancement of entrainment by cloud evaporation. These adjustments are consistent across both RCM-DEF-UW and RCM-DEF-Holtslag experiments. Its significant to highlight that the implications from the tropical deforestation simulations, especially the insights from the second design experiment (RCM-DEF-UW), represent novel contributions of the ICTP-RegCM model, that haven't been addressed in prior research, as communicated in Lodh (2021). The simulation length and initial condition for both the sets of control (RCM-CONTROL-UW, RCM-CONTROL-HOLTSLAG) and design (RCM-DEF-UW, RCM-DEF-HOLTSLAG) experiments is 00 UTC of 1st October 1999 to 00 UTC of 1st January 2011, where a spin-up time of 1 year and 3 months is neglected to mitigate errors due to initial values. While performing the design experiments (using the RegCMv4.4.5.10 simulations) the combination of physical parameterization schemes employed are the same as in control simulations (for details, refer to Table 1). The experiments are run continuously around the year from 00 UTC of 1st October 1999 to 00 UTC of 1st January 2011 using six hourly NCEP/NCAR-2 reanalysis data as boundary forcing (Kanamitsu et al. 2002) and Reynolds weekly SST (Reynolds et al. 2002). In both the control and deforestation design experiments, the RegCMv4.4.5.10 model employs a 30-s time step. The time step for the BATS land surface model is 600 s. Every 30 min, the radiation model is invoked, and emission computations are carried out every 18 h. This aligns with the model configuration described in Lodh (2021) where impact of extended desertification was studied.

This research study offers new perspectives on the impacts of tropical deforestation, leveraging the RegCMv4.4.5.10 model in conjunction with two PBL schemes. To assess the

Table 2 BATS vegetation table for the deforestation design experiment (*Source* ICTP RegCM Version 4.4 User Manual; Elguindi et al., 2014)

	Short Grass
Roughness length (m)	0.05
Min stomatal resistance (s/m)	60
Vegetation albedo for Wavelengths < 0.7 μ m	0.10
Vegetation albedo for Wavelengths > 0.7 μ m	0.30
Maximum fractional vegetation cover	0.85
Maximum leaf area index	6
Minimum leaf area index	0.5

significance of the changes in precipitation (and other meteorological variables) resulting from the deforestation of tropical rainforests, the Wilcoxon's nonparametric signed rank test is performed. The Wilcoxon Signed Rank Test computes the sum of ranks for positive and negative differences after ranking the differences between matched observations in absolute values. The lesser of these two sums is subsequently taken into consideration to establish the test statistic. The null hypothesis assumes that the median of the differences is zero, indicating no systematic shift between the paired samples. If the calculated test statistic falls within a critical region, determined by the chosen significance level, the null hypothesis is rejected, suggesting a significant difference between the paired samples (Lodh 2021). Hence, the objective, of the design experiment is to enumerate the effects of "tropical deforestation" on the ISM precipitation, circulation, surface fluxes, and other meteorological variables.

3 Results and discussion

The rainfall climatology for the JJAS (June, July, August, September) season across India, based on 10 years of data (2001–2010) sourced from IMD, TRMM observations, and the RegCMv4.4.5.10 model, are depicted in Figures S1 and S2 (from here on, figures labeled with 'S' can be found in the supplementary material). Figure S1 displays the spatial distribution of rainfall during the JJAS period, with the highest rainfall concentrations in the Western Ghats and north-east India. In contrast, the least rainfall is seen over north-west India. The RCM-CONTROL-UW model proficiently reproduced actual rainfall distribution across all studied regions, except northeastern India and the southern peninsula, where the rainfall level is higher than the IMD climatology.

The accuracy and verification of rainfall, temperature, and soil moisture measurements produced by the RegCMv4.4.5.10 model was previously established in Lodh (2021). Figure S2 also depicts that the rainfall bias with respect to TRMM observations falls within the range of -1 to -2 mm/day over the monsoon core region of India (MCRI), which is located in central India. Concurrently, the JJAS mean surface temperature bias (Figure S3) over MCRI ranges from $+0.5$ to 2 °C (Lodh 2021). The sensitivity of the atmospheric circulation and precipitation in the lower and middle troposphere over the Indian monsoon domain region to the tropical deforestation has been examined through anomalies of wind at 850 hPa and 500 hPa, moisture transport (MT) fluxes, precipitation, 500-hPa vertical velocity, surface fluxes, near surface air temperature, soil wetness, albedo etc. for monsoon JJAS season.

The control experiments are classified into two distinct types: RCM-CONTROL-UW and RCM-CONTROL-Holtslag. Analogously, the design experiments have their respective categorizations as RCM-DEF-UW and RCM-DEF-Holtslag for each simulation set. Here and in the subsequent section describing tropical deforestation results, anomaly is defined as the difference fields (design-control) between the corresponding fields. In the three panel figure the top panel is "Control" experiment run, middle panel is "design" experiment run and bottom panel is "anomaly (design-control)" with positive anomaly in "blue" and negative anomaly in "red" shades.

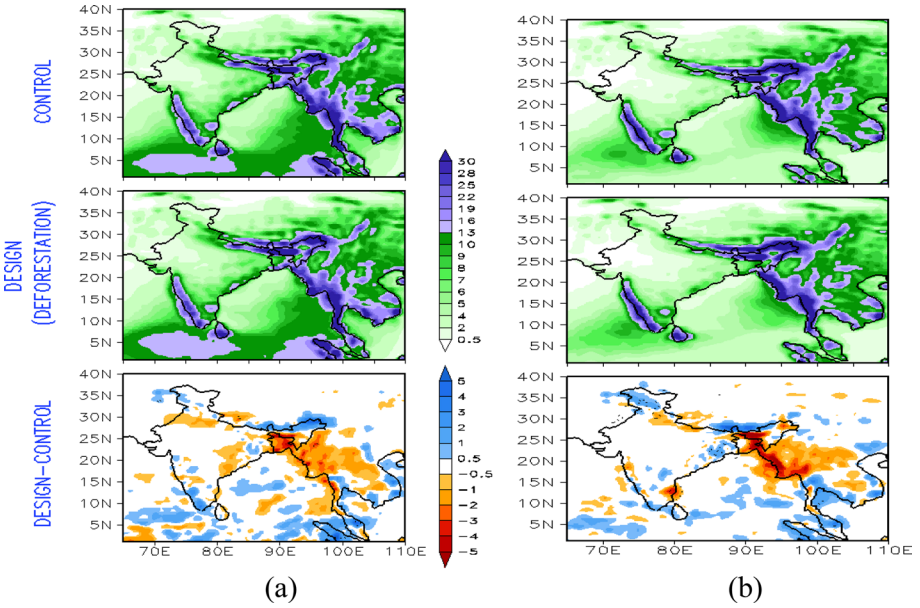

Fig. 2 The JJAS (2001–2010) composite precipitation (mm/day) and anomaly (design-control) for deforestation (**a**) RCM-DEF-UW (**b**) RCM-DEF-Holtslag, design experiments, respectively. (*The regions where there is decrease in precipitation is significant at 99% confidence level)* [*(top) CONTROL exp, (middle) DESIGN exp; and (bottom) anomaly (design-control)]

3.1 Effect of tropical deforestation on mean ISM meteorology

The tropical deforestation design experiment is to test the role and importance of vegetation along principal axis of monsoon travel (Krishnamurti and Bhalme 1976). Figure 2 shows the JJAS (2001–2010) mean precipitation (mm/day) and anomaly (design-control) for deforestation (a) RCM-DEF-UW (b) RCM-DEF-Holtslag, design experiments, respectively. Seasonal mean JJAS precipitation is decreasing by approximately −2 mm/day (i.e. ~ 30% less w.r.t control run, $p < 0.01$), over north-east India, western Himalayan region of north India, Chennai and its nearby locations of peninsular India and Indonesia, Thailand and Myanmar regions of the South-east Asia dur to tropical deforestation. It is important to mention here that both the RCM-DEF-UW and RCM-DEF-Holtslag design experiments are for capturing the impact of tropical deforestation within the scope of the RegCMv4.4.5.10 model. All the parameterization schemes to run the RCM-DEF-UW and RCM-DEF-Holtslag model are the same except, UW PBL scheme is used to represent boundary layer processes in first design experiment whereas Holtslag PBL scheme is used in the second design experiment.

Figure S4 and S5 shows the probability distribution functions of annual precipitation (mm/day) over central India from the Control (RCM-CONTROL-UW) and deforestation (RCM-DEF-UW) design experiments. The mean precipitation over central India and north-west India is decreasing by −6.2 mm/day and −3.4 mm/day, respectively over the period 2001–2010 due to deforestation. Also, the precipitation variability is decreasing due to tropical deforestation implemented in the RCM. Figures 3, 4 show the anomalous wind at 850 hPa and 500 hPa level during JJAS season and it can be concluded that magnitude

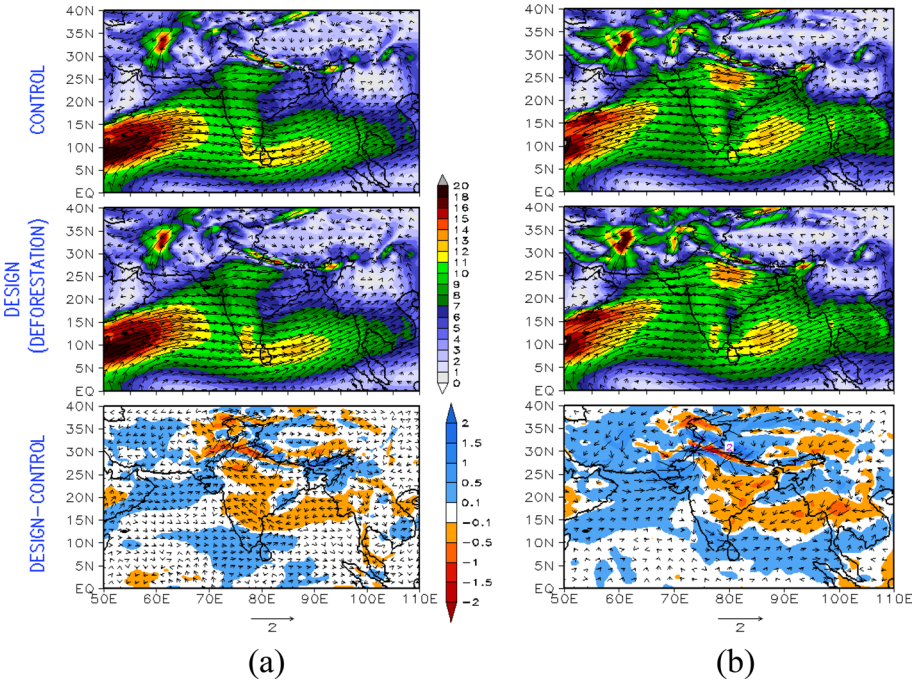

Fig. 3 The JJAS (2001–2010) composite mean and anomaly (design-control) of wind (m/sec) and change in direction at 850 hPa for deforestation (**a**) RCM-DEF-UW (**b**) RCM-DEF-Holtslag, design experiments, respectively

of wind has decreased over South-east Asia, Bay of Bengal (BOB) and central India region with a tendency to form anomalous anticyclonic circulation at 850 hPa extending up to 500 hPa, in both the RCM-DEF-UW and RCM-DEF-Holtslag simulations. The subsidence during JJAS season has increased over east India, Bangladesh and the maritime subcontinent wherever deforestation is implemented in the model, as seen in Fig. 5. The anomalous positive values of 500-hPa vertical velocity, represents subsidence. From Fig. 6, it is observed that MT at 850 hPa, has decreased over South-east Asia, BOB, Eastern Ghats, Bengal and western Himalayan region of north India. It is important to note here that due to tropical deforestation, the direction of the anomalous flow in MT is opposite to the direction of mean JJAS monsoon flow. The decline in monsoon precipitation over India due to tropical deforestation can be linked to reduction in MT at 850 hPa, vertically integrated moi sture transport flux upto 300 hPa (Figure S6) over north India, Bay of Bengal (BOB) and its neighboring land region over south-east Asia (approx. by -15 kg/m/sec). Due to deforestation the meridional component of vertically integrated moisture transport flux is reduced over South-east Asia, BOB and north India, whereas the zonal component of the vertically integrated moisture transport flux is reduced along the principal axis of monsoon, including the BOB region (Figure S6). Accompanying this reduction in MT, due to deforestation there is an increase in the height of the lifting condensation level (Figure not shown) over India by 15%, in the deforestation experiment compared to the control. Thus, tropical deforestation inhibits formation of clouds over the Indian sub-continent. Figure 7 explicitly showcases a divergence in the water vapor flux spanning the entire column

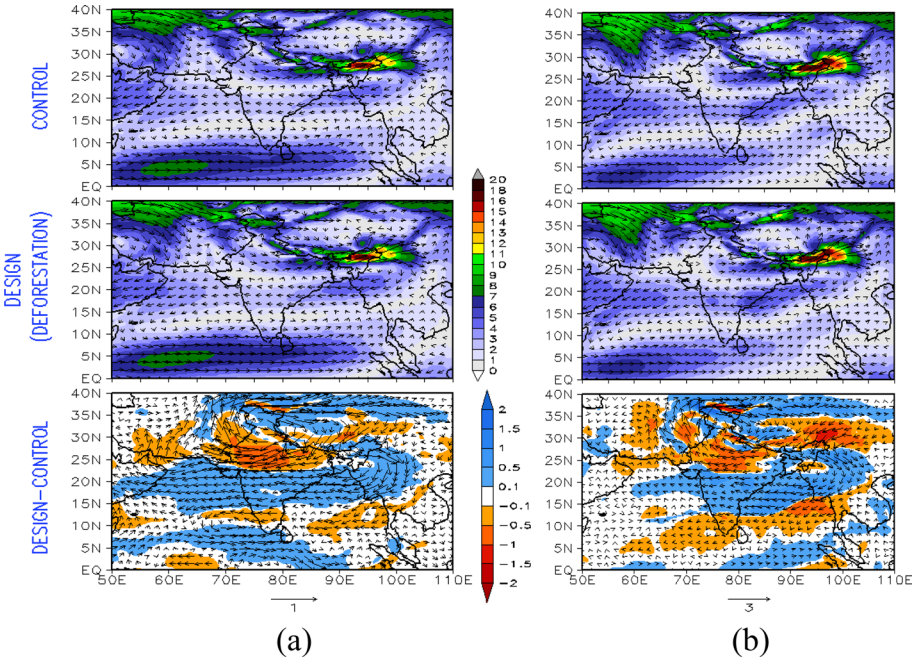

Fig. 4 The JJAS (2001–2010) composite wind (m/sec) anomaly (design-control) and change in direction at 500 hPa for deforestation (**a**) RCM-DEF-UW (**b**) RCM-DEF-Holtslag, design experiments, respectively

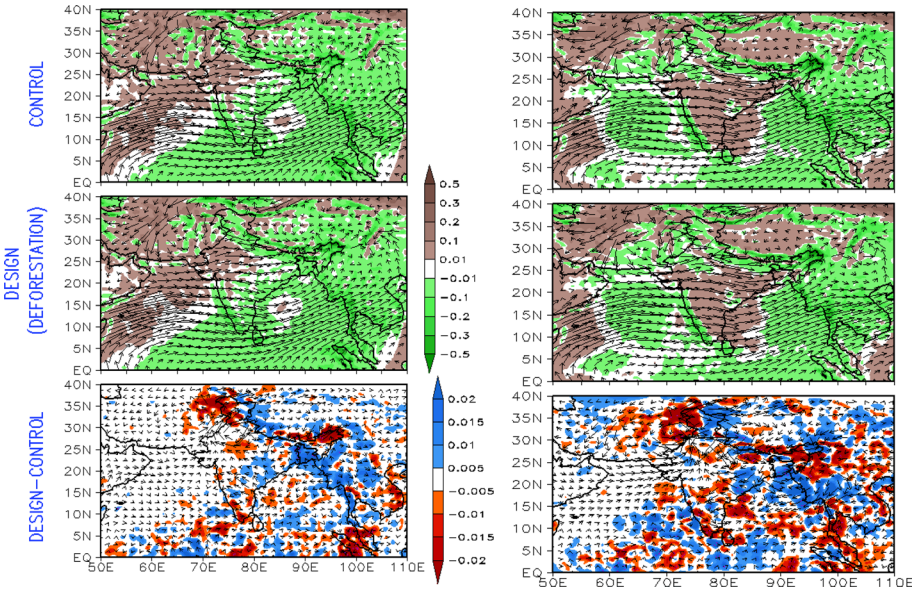

Fig. 5 The JJAS 850-hPa wind ($msec^{-1}$) and 500-hPa vertical velocity (hPa/sec; shaded, positive values representing subsidence) anomaly (design-control) for deforestation (**a**) RCM-DEF-UW (**b**) RCM-DEF-Holtslag, design experiments, respectively

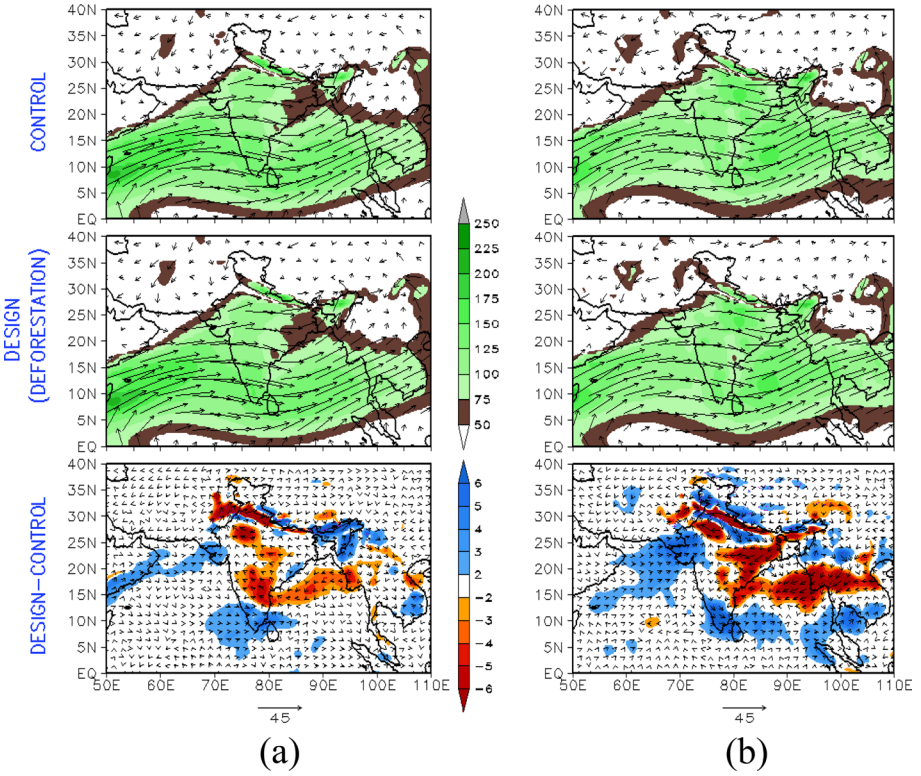

Fig. 6 The JJAS (2001–2010) composite mean and anomaly (design-control) of moisture transport at 850 hPa (kg/m/sec) for deforestation (**a**) RCM-DEF-UW (**b**) RCM-DEF-Holtslag, design experiments, respectively

up to 300 hPa, covering India and the maritime subcontinental region (with a significance level of $p < 0.01$). This divergence further contributes to the observed decrease in JJAS precipitation. It is worth noting that in this context, negative values linked with the convergence of vertically integrated water vapor flux indicate convergence, while positive values denote the divergence of water vapor flux. Therefore, tropical deforestation induces a displacement in water vapor over the primary monsoon axis. This leads to a shift in both the amount of precipitable water (Figure S7) and the moisture flux on a regional scale over the region under the principal axis of Asian monsoon.

The Monsoon Hadley Index has shown a noticeable decline of approximately −1.2% per decade from 2001 to 2010, in tropical deforestation experiment in comparison to the control experiment (Fig. 8). This is evident for both RCM-DEF-UW and RCM-DEF-Holtslag design experiments. Consequently, the deforestation along the primary axis of monsoon destabilizes the wind patterns of the Indian monsoon up to 500 hPa. Other metrics such as near surface air temperature, SHF, soil wetness, LHF and evaporative fraction for the Control (RCM-CONTROL-UW) and deforestation (RCM-DEF-UW) design experiments are represented in Figs. 9, 10, 11, 12, 13. As a consequence of deforestation there is increase in near surface (2 m) air temperature over Indo-Gangetic plains, north, east and north-east India and some regions in south-east Asia, as depicted in Fig. 9. Over the

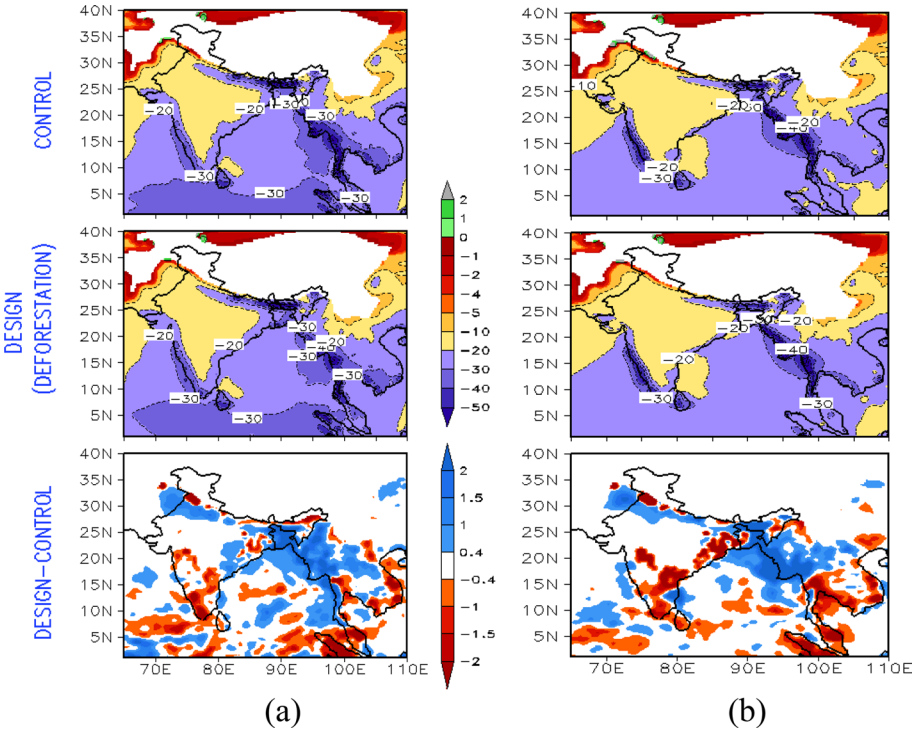

Fig. 7 The JJAS (2001–2010) composite mean and anomaly (design-control) of convergence of vertically integrated water vapor flux (mm/day) for deforestation (**a**) RCM-DEF-UW (**b**) RCM-DEF-Holtslag, design experiments, respectively

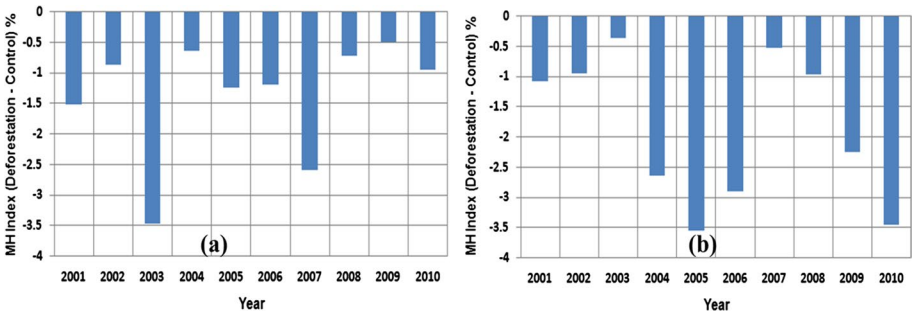

Fig. 8 Sensitivity of Monsoon Hadley (MH) index as calculated for deforestation (**a**) RCM-DEF-UW (**b**) RCM-DEF-Holtslag, design experiments, respectively

maritime sub-continent, near surface air temperature increases only in the RCM-DEF-UW design experiment. The SHF has increased by + 40 Wm^{-2} ($p < 0.01$) over the whole of the tropical rain-belt of south and south-east Asia, i.e., from India to Thailand and Cambodia (Fig. 10). There is increase in Bowen's ratio over north-west India due to tropical deforestation (Figure S8). This temperature shift can be attributed to the escalation in SHF, which is prominently observed across the tropical rain-belt, extending from India through to the

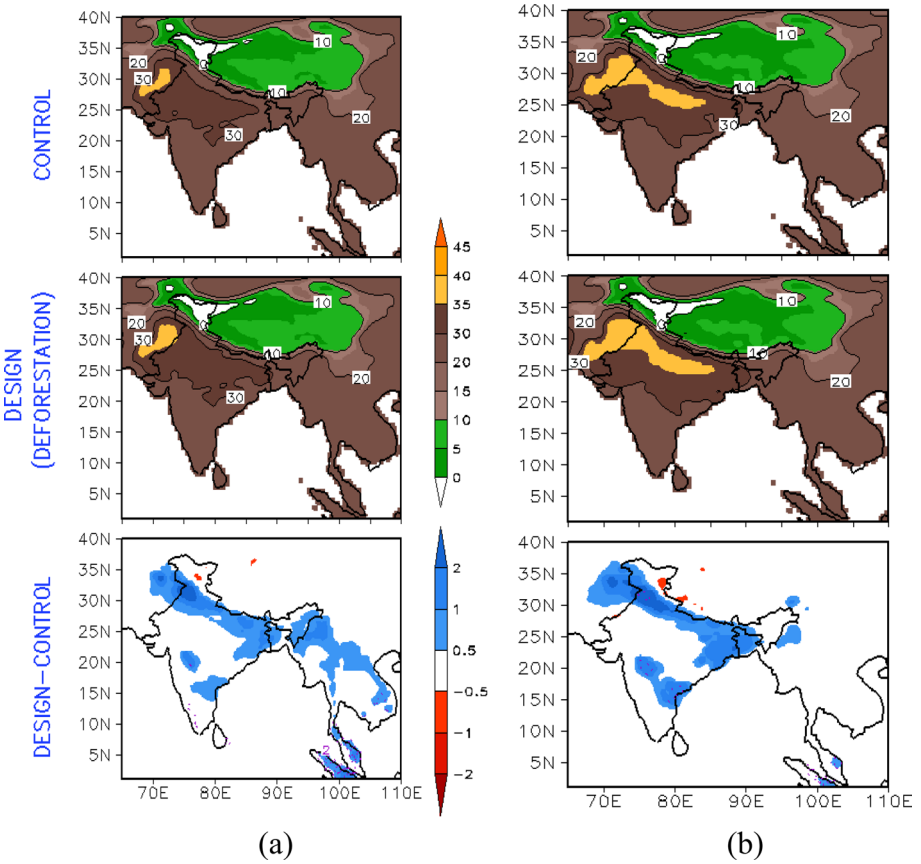

Fig. 9 The JJAS (2001–2010) composite mean and anomaly (design-control) ($p < 0.01$) of near surface air temperature at 2 m (°C) for deforestation (**a**) RCM-DEF-UW (**b**) RCM-DEF-Holtslag, design experiments, respectively

regions of Thailand and Cambodia in Southeast Asia, as shown in Figs. 9, 10 (Boysen et al. 2020). There is decrease in surface soil moisture and LHF over south-east Asia, Eastern Ghats, Western Ghats, peninsular India, Indo-Gangetic plain and north India, is highlighted in Figs. 11, 12. Due to deforestation the evaporative fraction (Fig. 13) and recycling ratio (Figure not shown) has also decreased over the Indian subcontinent and nearby areas. Tropical deforestation leads to a decline in precipitation recycling due to reduction in soil moisture and evapotranspiration, especially over the primary monsoon regions of India and Southeast Asia during the summer monsoon months (JJAS). Thus, the region of changes in the near surface parameters in the RCM-DEF-UW and RCM-DEF-Holtslag, design experiments, is synonymous with the regions where tropical deforestation is done in the model. Thus, an impact of tropical deforestation on near surface temperature over Indian sub-continent is clearly derived from this study.

In the deforested zones, there's a noticeable increase in upward longwave energy flux, ranging between + 20 to + 40 Wm^{-2}, as depicted in Fig. 14. The albedo also increases by 0.05 units (Fig. 15), which is also reported in similar studies (Mabuchi et al. 2005, Mabuchi 2011; Strandberg et al. 2023) on vegetation change. Conversely, there's a reduction in

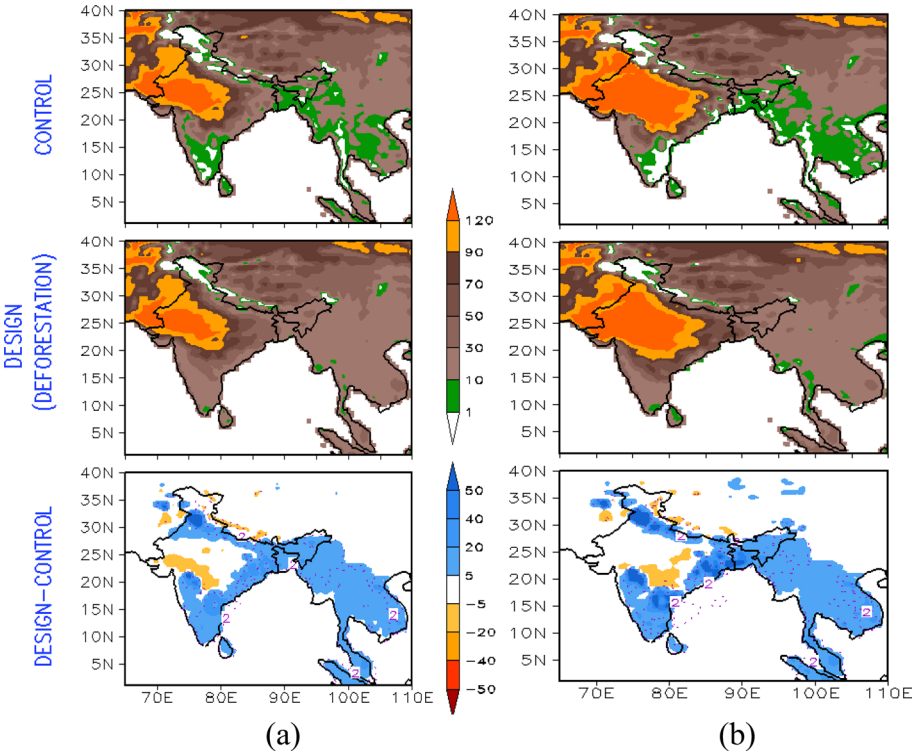

Fig. 10 The JJAS (2001–2010) composite mean and anomaly (design-control) of sensible heat flux (Wm^{-2}) for deforestation (**a**) RCM-DEF-UW (**b**) RCM-DEF-Holtslag, design experiments respectively

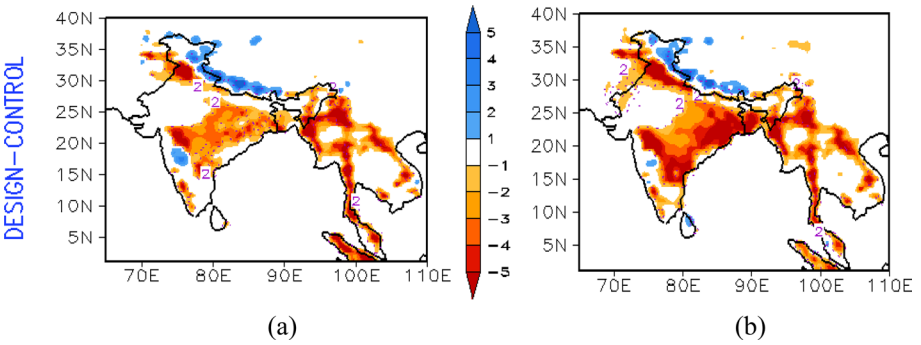

Fig. 11 The JJAS (2001–2010) composite mean and anomaly (design—control) ($p < 0.01$) of soil wetness (mm) for deforestation (**a**) RCM-DEF-UW (**b**) RCM-DEF-Holtslag, design experiments, respectively

net radiation at the surface by approximately −5 to −40 Wm^{-2}. Net radiation, in this context, is the sum of net upward longwave energy flux and net downward shortwave energy flux, which is calculated as (SWin − SWout + LWin − LWout), as illustrated in Fig. 16. The pattern of albedo alteration corresponds with the changes in net radiation, though with an inversion in polarity. Moreover, it has been observed that the regions subjected to

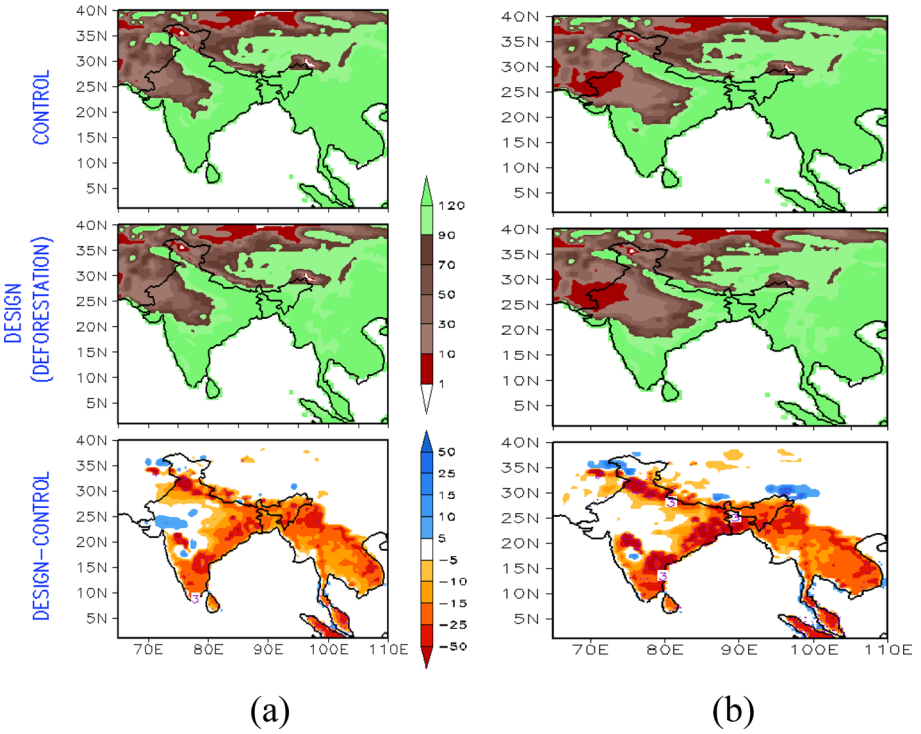

Fig. 12 The JJAS (2001–2010) composite mean and anomaly (design-control) of latent heat flux (Wm^{-2}) (**a**) RCM-DEF-UW (**b**) RCM-DEF-Holtslag, design experiments, respectively

deforestation within the model see an increase in surface upward longwave-radiation flux (as corroborated by Sud et al. 1988, 1996; Eltahir 1996; Zheng and Eltahir 1997; Durieux et al. 2003; Sen et al. 2004; Li et al. 2016). Generally, an increase in OLR indicates cooling of the atmosphere or the atmosphere becoming drier or less conducive to cloud formation resulting in decrease in precipitation. Its important to note the sign convention used in this study: the direction of surface downward shortwave energy flux moving from the atmosphere to the land surface is taken as positive. On the other hand, the direction of surface upward longwave energy flux transferring from the land surface to the atmosphere is considered negative. This is attributed to lower surface roughness, as surface warming and anomalous increase in sensible heating. Hence, decreased evapotranspiration, increase in net upward longwave flux, Bowen's ratio, SHF lead to a warmer, higher and drier planetary boundary layer ($p < 0.01$; Figure S9. Thus, due to tropical deforestation over a dry surface the rate of ascent of the boundary-layer top and deepening of the convective boundary layer tends to be faster, with negative feedback of rainfall with soil moisture. Bhowmick and Parker 2018 also predicts the same using theoretical framework just that the negative or positive feedback depends upon the atmospheric profile, Bowen's ratio (inversion) and convective instability parameter of the region. It is important to mention here that both the simulations, RCM-DEF-UW and RCM-DEF-Holtslag are unanimous in the deriving the conclusions from the deforestation experiments.

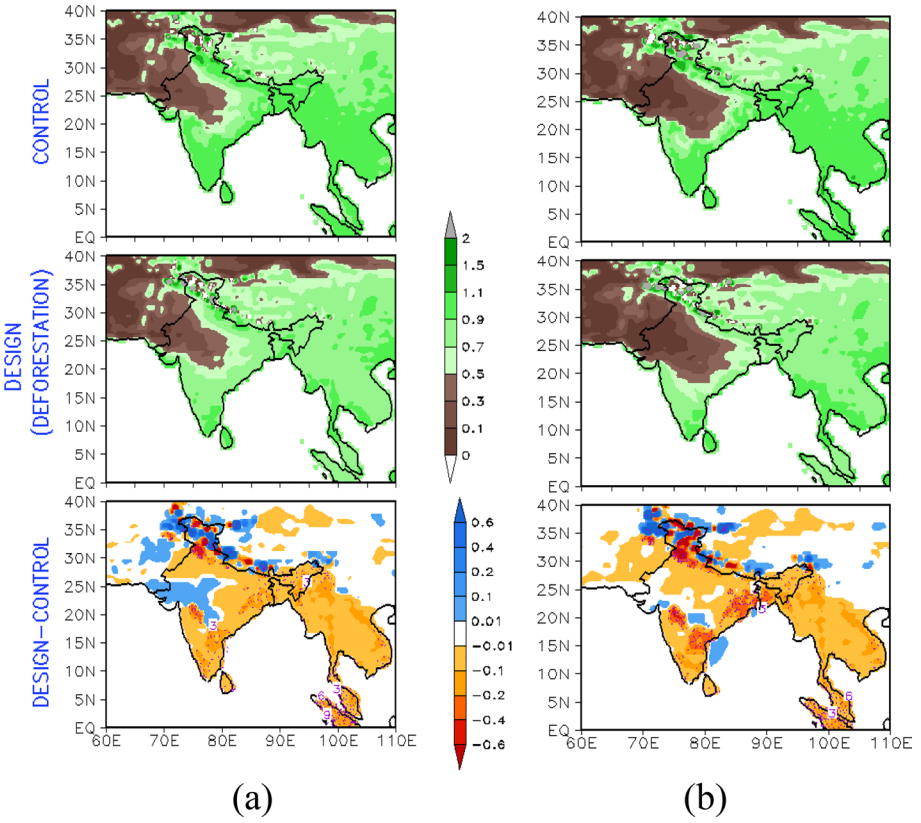

Fig. 13 The JJAS (2001–2010) composite mean and anomaly (design-control) of evaporative fraction for deforestation (**a**) RCM-DEF-UW (**b**) RCM-DEF-Holtslag, design experiments, respectively

The ISM precipitation appears to decrease due to tropical deforestation. One significant reason is the albedo increase, which exceeds a critical point of 0.03 (Dirmeyer and Shukla 1994). This deforestation leads to a notable decrease (increase) in net radiation and LHF (SHF). Such variations disrupt the radiative equilibrium over the Indian region, which, in turn, disrupts the ISM circulation, resulting in reduced ISM rainfall. This observation aligns with the conclusions drawn by studies by other researchers although their focus was on different global locations (Charney 1975; Charney et al. 1975, 1977; Ripley 1976; Shukla and Mintz 1982; Zeng and Neelin 1999; Zickfeld et al. 2005).

3.2 Statistical analysis of tropical deforestation design experiment

This section covers the statistical analysis of tropical deforestation using the RegCMv4.4.5.10 model in conjunction with the BATS vegetation module. The influence of the deforestation design experiment is examined through the substitution of forested areas with the "short grass" type of vegetation, characterizing deteriorated pastures, within the context of the "Control" vegetation map. The tropical deforestation design experiment entails methodical adjustment of the albedo, roughness length, and hydrological characteristics of the surface. This is achieved by modifying the model's namelist file, utilizing

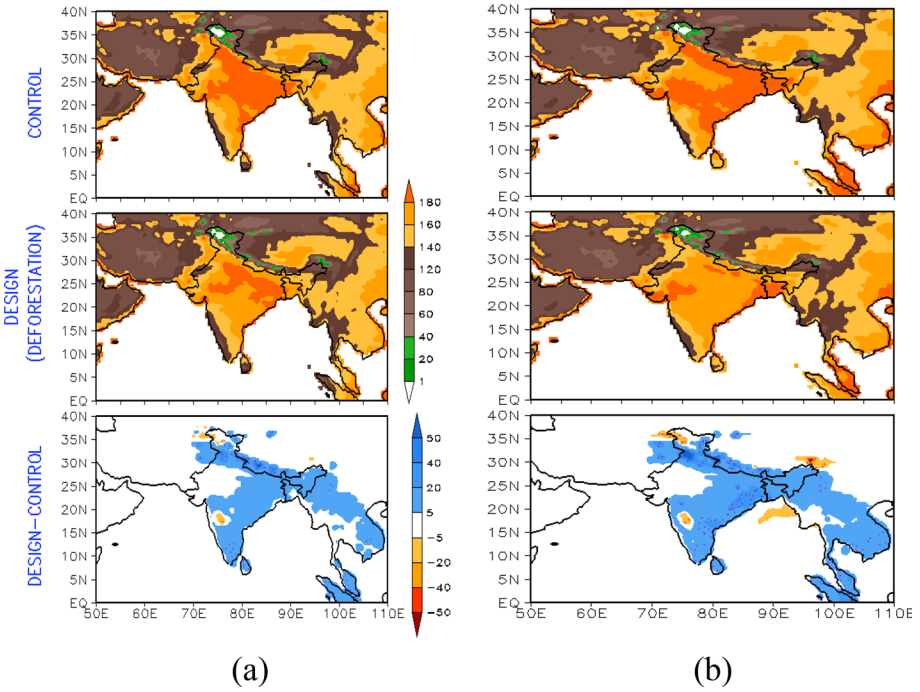

Fig. 14 The JJAS (2001–2010) composite mean and anomaly (design-control) of net upward longwave energy flux (Wm^{-2}) for deforestation (**a**) RCM-DEF-UW (**b**) RCM-DEF-Holtslag, design experiments, respectively

a "fudge" parameter set to "true," and introducing the updated land-use map that accounts for tropical deforestation. The experimentation spans a duration of 11 years, wherein the analysis primarily focuses on the decade following a spin-up phase of 1 year and 3 months. Throughout the experimental phase, actual sea surface temperature (SST) data is incorporated, including significant El Nino and La Nina events. In order to assess the significance of the outcomes, the Wilcoxon rank sum statistical test (Lodh 2021; Lorenz et al. 2016) is applied to the anomalies of the 10 JJAS (June to September) months for both the control and deforested design experiment runs (as depicted in Figure S10). The anomalies for the JJAS months are calculated by taking the difference between the JJAS monthly figures from the control run and those from the experimental design run. We assume that these monthly anomalies are statistically independent, based on the justification that the autocorrelation time frames within the samples don't exceed one month. The observations in this segment echo the earlier results from Sect. 3.1. It is evident that variations in precipitation, SHF, LHF, and the convergence of the integrated water vapor flux are not only consistent with the previous findings but also statistically noteworthy with a significance level of $p < 0.01$.

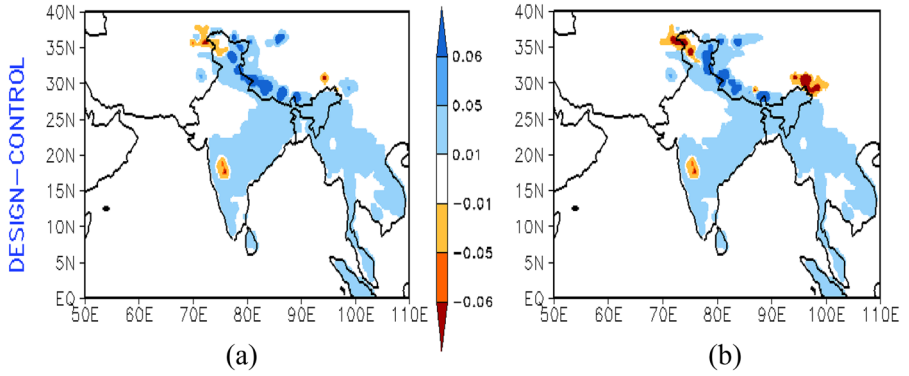

Fig. 15 The JJAS (2001–2010) composite mean and anomaly of albedo (design-control) for deforestation (**a**) RCM-DEF-UW (**b**) RCM-DEF-Holtslag, design experiments, respectively

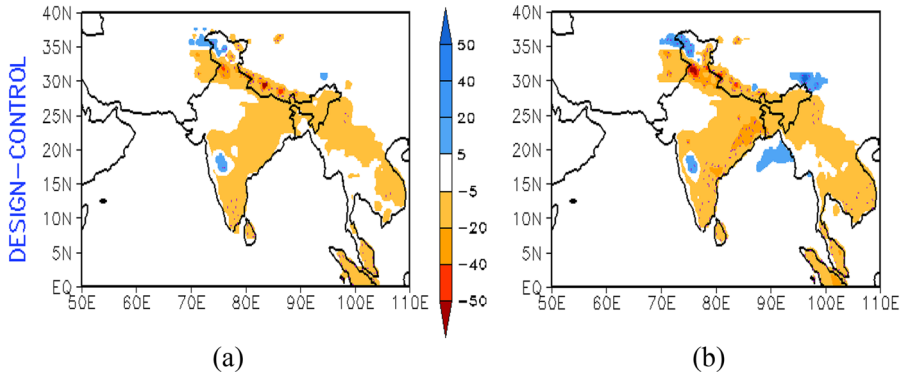

Fig. 16 The JJAS (2001–2010) composite mean and anomaly ($p < 0.01$) of net radiation (W/m^{-2}) anomaly (design-control) (positive is downward) for deforestation (**a**) RCM-DEF-UW (**b**) RCM-DEF-Holtslag, design experiments, respectively

3.3 Effect on variability of mean precipitation and surface fluxes

This section addresses the land–atmosphere feedback arising from tropical deforestation through fluctuations (measured as standard deviation) of the ISM rainfall, latent and sensible heat transfers (Ferranti et al. 1999). For this purpose, data is collected from each grid point, spanning both the control study and the design experiments that simulate tropical deforestation. Figures 17(a–f) map out the standard deviations pertaining to precipitation, LHF and SHF, as observed in both control and deforestation scenarios. A consistent pattern of precipitation variability is evident from Fig. 17a and b for both setups. Intriguingly, in months of May and June, in the control simulations there's a pronounced fluctuation in rainfall (i.e. variability in rainfall) especially over regions like the Western Ghats, north-east India and Himalayan foothills extending upto north-west India. In the experiments simulating tropical deforestation, there's a noticeable decrease in rainfall variability (both strength and spread) over northwest India during May and July. This suggests that tropical deforestation adversely impacts the variability of the Indian monsoon, particularly

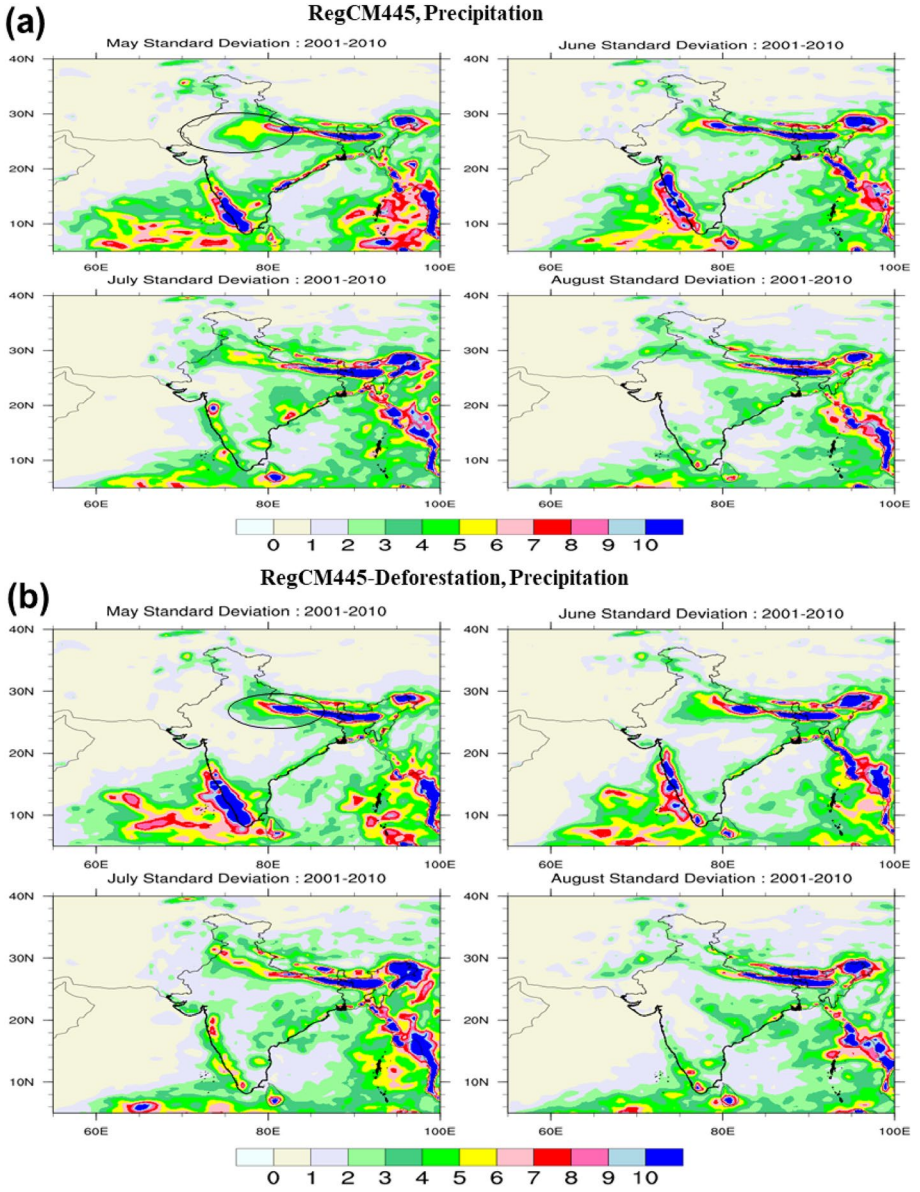

Fig. 17 Standard deviation of monthly rainfall in (**a**) baseline/control experiment (**b**) deforestation design RCM-DEF-UW experiment, **c** and **d** same as in (**a** and **b**) but for latent heat flux (LHF), **e** and **f** same as in (**a** and **b**) but for sensible heat flux (SHF)

its movement towards the northwest. Also, the consistency of surface energy fluxes, notably LHF, is diminished over areas like the Indo-Gangetic plains and central India due to such deforestation. The SHF variability also experiences a drop, especially in the monsoon trough area that stretches from central India towards the north and north-west. As a result, reductions in surface fluxes, integral to the energy budget, simultaneously influence

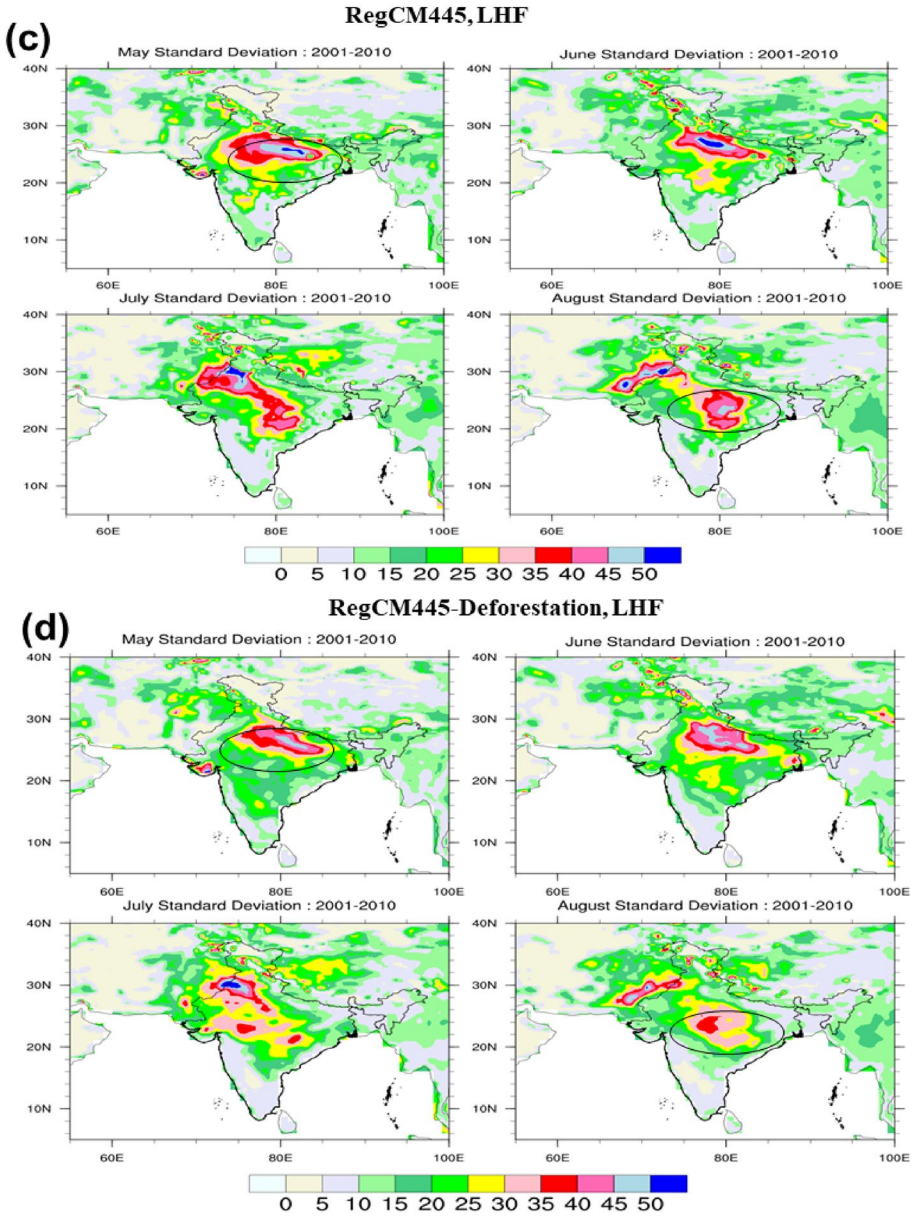

Fig. 17 (continued)

terrestrial parameters (Yuan et al. 2021). These parameters include soil moisture, evapotranspiration processes, types of vegetation, and overall ecosystem dynamics. Consequently, this plays a significant role in shaping the precipitation variability, as indicated by studies from Pielke et al. 1998 and Ferranti et al. 1999. Terrestrial coupling index of 2 m-temperature and atmospheric coupling index of PBL (Lodh 2020) is also calculated for the two control experiments (RCM-CONTROL-UW and RCM-CONTROL-Holtslag)

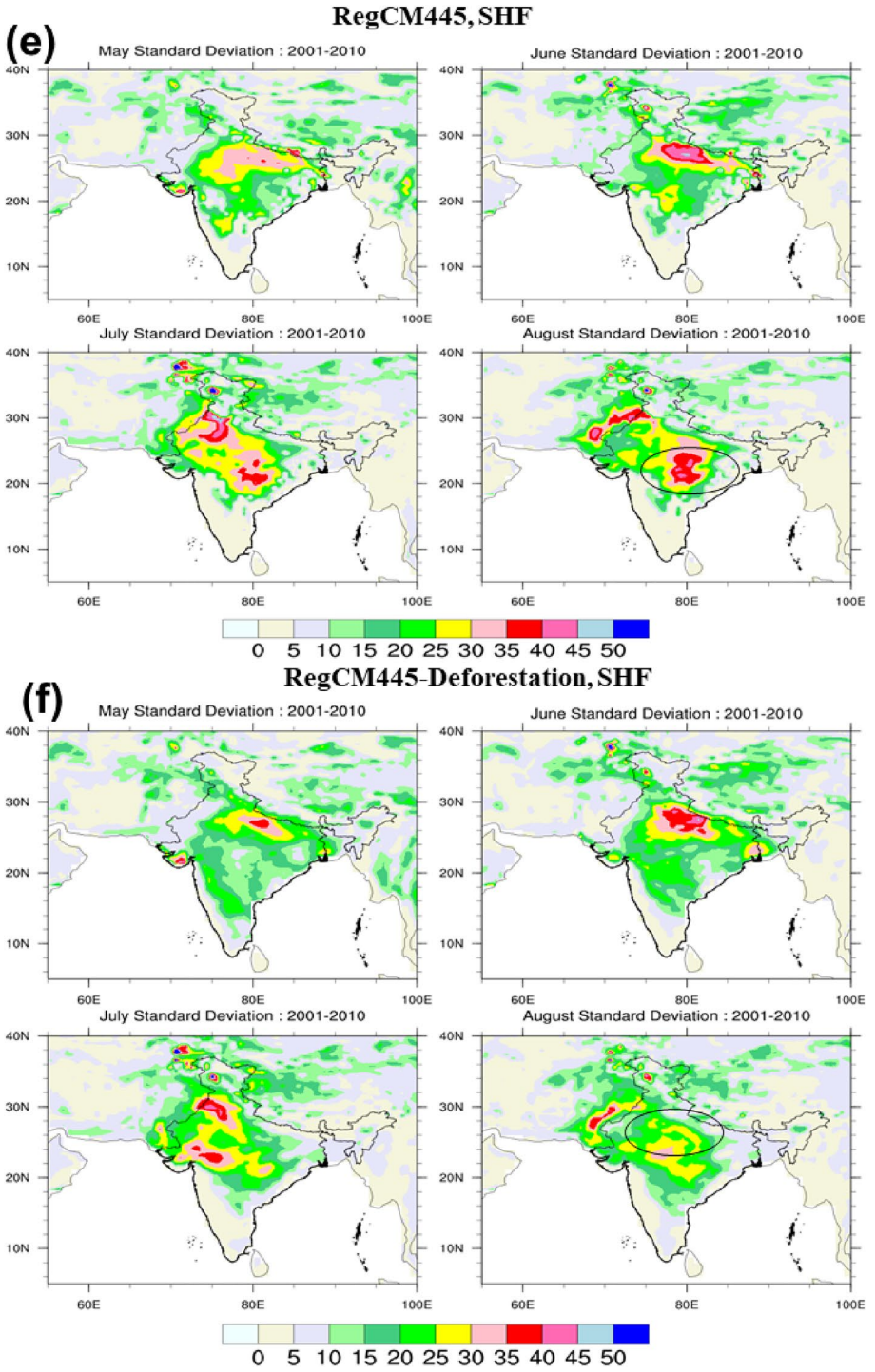

Fig. 17 (continued)

for the time period May to September 2001–2010 (Figures S11 and S12). Over central India and north-west India, the value of terrestrial coupling index of 2 m-temperature and SHF ranges between 30–45 W m^{-2} in the RCM-CONTROL-UW and RCM-CONTROL-Holtslag simulations. However, the strength and domain of extent of coupling is larger in the RCM-CONTROL-Holtslag simulations. This is because the standard deviation (or variability) in SHF is more in the RCM-CONTROL-Holtslag simulations than RCM-CONTROL-UW. The atmospheric coupling index of SHF and PBL across central and CI and north-west Indian sub-continent with values ranging between 150 and 250 m (200 and > 250 m) in the RCM-CONTROL-UW (RCM-CONTROL-Holtslag) simulations (Figures not shown). Furthermore, the deforestation design experiments reveal heightened shifts in land–atmosphere interactions over northwestern India in terms of coupling between 2 m-temperature to SHF to PBL, abating (strengthening) the latent (sensible) heat feedbacks of land–atmosphere and convective activities in the region.

3.4 Effect on dominant modes of variability of precipitation, soil moisture and surface fluxes

This section explores into the impact of feedback, triggered by tropical deforestation, on the primary three modes of variability observed in precipitation, soil moisture, LHF and SHF. The variance percentage linked to each empirical orthogonal function (EOF) is marked at the top right of each corresponding graph, as seen in Figures S13, S14, S15, S16. The figures from the control, RCM-CONTROL-UW and tropical deforestation, RCM-DEF-UW design experiment is reported here. In the design experiment simulating tropical deforestation (see Figure S13), the spatial layout of EOF1 for precipitation largely mirrors its counterpart in the control, accounting for roughly the same variance (~67.8%). EOF1's peak variability can be pinpointed over areas like the Western Ghats and north-east India, which are regions of substantial rainfall during the JJAS season over India. Turning to the control setup, as depicted in Figure S13(a and b), the spatial layout for EOF2 highlights positive rainfall anomalies over regions like Western Ghats and north-east India, while negative anomalies are evident over the foothills of Himalaya. This distribution signifies the typical positioning of the tropical convergence zone in line with both the active and break cycles of the monsoon. Active monsoon phases align with positive time coefficients of EOF2 precipitation, whereas negative values point to subdued monsoon phases, as detailed by Ferranti et al. 1999. For the tropical deforestation design experiment, the spatial outline of EOF2 prominently features peaks where the control experiment's EOF2 has troughs. This suggests that alterations in land use due to tropical deforestation reshape the second dominant mode of precipitation variability. Similarly, the spatial representation of EOF2 for soil moisture (Figure S14) within the tropical deforestation design experiment underscores the repercussions of deforestation-driven changes in land use and cover on the variability of soil moisture, starting from the second mode. The positive time coefficients for both EOF2 and EOF3 in soil moisture, which account for variability percentages of roughly 6% and 4.5% respectively, distinctly demonstrate the influence of tropical deforestation on soil hydration in areas that lie along the monsoon's main trajectory. A consistent pattern emerges when evaluating the impact of deforestation on the second and third dominant variability modes for LHF (with roughly 7% variability) is depicted in Figure S15. Whereas from Figure S16, the second mode of variability in SHF (with roughly 9% variability), depicts the impact of deforestation on SHF, implying impact of LULC change on land surface fluxes.

4 Conclusion

Numerical simulations assessing changes in LULC (tropical deforestation) were conducted utilizing the ICTP RCM version RegCMv4.4.5.10. The RegCMv4.4.5.10 simulations effectively determine the model's capability to replicate the climate conditions in India. Also, the technique to implement "tropical deforestation" in the RegCMv4.4.5.10 model was able to isolate the mechanisms that drive the development of meteorological events in event of tropical deforestation. This study quantitatively demonstrates the impact of tropical deforestation on the alteration of rainfall, temperature, and atmospheric circulation over Indian subcontinent and its nearby regions (regions lying over the principal axis of Asian monsoon). These anomalies impact the local hydro-climate, leading to drought-like conditions, further decreasing the intensity and duration of monsoon rain, forming an irreversible hysteresis loop. This confirms the existence of teleconnection effects due to tropical deforestation. To investigate the influence of tropical deforestation design experiments, two distinct simulation sets were executed:

- Control simulation using the USGS natural land use map as its foundation.
- A design simulation that employs a modified land use map, specifically tailored to replicate the effects of deforestation.

The results of the tropical deforestation design experiments were assessed for versatility by employing two unique combinations of PBL parameterization schemes: the Holtslag PBL and the University of Washington Turbulence closure PBL. Both of these were integrated with the RCM. For convection processes, the Emanuel convection scheme was applied over land, while the Grell scheme was used over the ocean, incorporating the Arakawa Schubert 1974 closure. The key findings of these experiments are outlined as follows:

i. Due to tropical deforestation, the JJAS precipitation over India, Indo-Chinese peninsula and the maritime sub-continent, along the principal axis of the Asian monsoon, experience a statistically significant decrease. The observed reduction is ascribed to the emergence of an anomalous anti-cyclonic circulation over eastern India, a consequence of tropical deforestation. This results in diminished convective heating, leading to a notable drop in precipitation when contrasted with the control experiment. Moreover, the anomalous anti-cyclonic flow that forms over the northern sector of the Bay of Bengal due to tropical deforestation curtails moisture advection and the vertically integrated moisture flux upto 300hPa, effectively diverting moisture away from adjacent areas, inhibiting the travel of atmospheric rivers. On land, the wind's intensity diminishes, and its direction reverses due to a decrease in surface roughness. The findings from this current research using the RegCMv4.4.5.10 model corroborates these observations, highlighting both local impacts and a decrease in the ISM rainfall. Furthermore, the recycling ratio decreases, resulting in a negative soil moisture feedback due to deforestation (Leite-Filho et al. 2021). As mentioned earlier in the tropical deforestation experiment, the decrease in surface pressure combined with decreasing wind magnitude leads to a calm but dry northwesterly wind over the Indian (land) region. This prevents moisture-laden southerly winds from moving towards land. The experiments focused on deforestation underscore that an increase in vegetation albedo and a decline in surface roughness (refer to Table 2) lead to

reduced solar radiation absorption on the surface. This results in a cooling effect, especially pronounced over northwestern India. This cooling narrows the temperature differential between land and sea, consequently impacting the north–south pressure gradient and the Indian monsoon's Hadley index. This shift means the easterly winds originating from the Bay of Bengal don't reach the mainland, which subsequently results in diminished precipitation inland. Hence, the elevation in albedo, attributed to the loss of vegetation, negatively and significantly impacts the evolution of the monsoon (ISM). Deforestation further influences the variability and the primary three Empirical Orthogonal Functions (EOFs) linked to the oscillation of the ISM. This influence manifests through alterations in surface energy fluxes, soil moisture content, evapotranspiration, and, consequently, rainfall across the Indian region (See Fig. 18). Its pivotal to recognize, however, that the effects of deforestation on precipitation patterns possess inherent uncertainties too.

ii. The experiments focusing on deforestation highlight that increases in albedo, owing to diminished plant cover, contributes to a decrease in JJAS soil moisture, evapotranspiration, and rainfall. This increase in albedo results in more radiation being reflected. Within the framework of the tropical deforestation design experiments, there is a noted average decline in precipitation by approximately − 2 mm/day. Concurrently, albedo surpassed the pivotal threshold value of 0.03. Albedo is an important factor, acting as a thermostat in regulating the climate's response to tropical deforestation. As deforestation affects tropical regions, there's a marked elevation in albedo, leading to the cooling of the surface. This cooling prompts a greater atmospheric subsidence, essential for sustaining long-wave radiation emission into the atmosphere. The decline in rainfall over a broader geographical area, beyond the region where deforestation occurs (i.e., teleconnection effects), is influenced by the higher albedo of deforested surfaces and the reduced evapotranspiration of crops and pastures compared to natural vegetation. Both from this study and previous literature it is found out that LHF, a significant factor in maintaining the recycling ratio, is considerably reduced by 25% due to deforestation. Any alteration in the lower boundary condition in a regional climate model (RCM) when paired with a decrease in vegetation (such as deforesta-

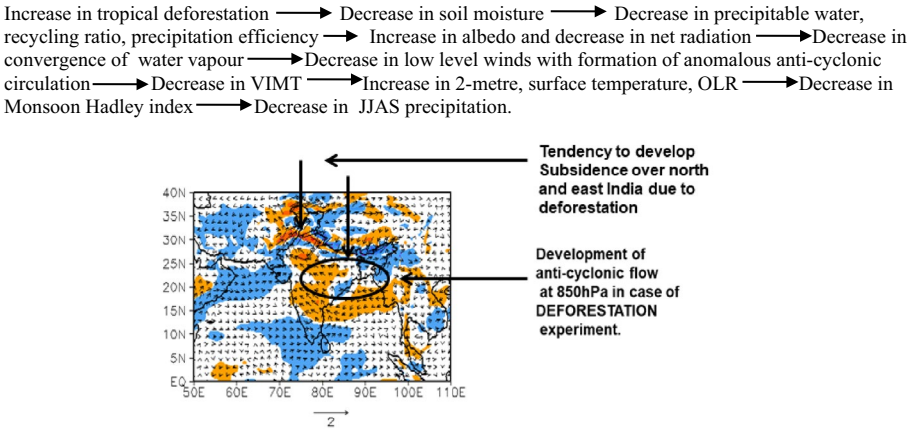

Fig. 18 Flowchart of the consequences of tropical deforestation experiment

tion or desertification) is further amplified by a reduction in rainfall, perpetuating heat wave and drought-like conditions.

iii. Precipitation plays a crucial role in the terrestrial and atmospheric water cycle, and repercussions of human-induced climatic shifts (anthropogenic climate change) such as tropical deforestation, on rainfall patterns hold profound consequences for farming practices, especially in the prime grain-producing regions of India. The increase in tropical deforestation over the hot spot regions of land–atmosphere like South-east Asia leads to alterations in precipitation over India through various mechanisms like alterations in soil moisture, evapotranspiration (ET), and energy fluxes over India. This transformation is facilitated by multiple pathways, including shifts in soil moisture, evapotranspiration (ET), and energy flux dynamics within India. A noticeable consequence is the diminished MT across the Bay of Bengal (BOB). Tropical deforestation leads to a decline in the total water content available in the atmosphere (precipitable water), the proportion of rainfall that returns to the atmosphere through evaporation (recycling ratio), and the efficiency with which rainfall is produced from available moisture (precipitation efficiency). In tandem, there's an increase in surface reflectivity (albedo) and a decrease in the net radiation received at the surface. This ultimately hampers the upward movement and convergence of water vapor, diminishing the propensity for low-level cloud formation. A secondary consequence is the weakening of low-level winds, promoting the development of an anti-cyclonic circulation pattern. In general, the results from the deforestation experiment reports that large-scale deforestation reduces net radiation at surface and the total heat flux by $\sim 20 \mathrm{Wm}^{-2}$.

iv. The alterations in LHF and MT combined with changes in the Monsoon Hadley index, have profound consequences on the water and energy cycles of the region. This results in a net reduction in summer monsoon (JJAS) rainfall over India. Furthermore, the increase in sensible heat flux (SHF), temperatures near the surface, and the increase in outgoing longwave radiation accentuate these shifts. Numerical analyses conducted using a regional climate model (RCM) reveal that tropical deforestation can amplify the effects of surface reflectivity (albedo) and evapotranspiration, leading to noticeable shifts in-ground and air temperature during the Indian monsoon by $+1$ to $+1.5$ °C. Consequently, higher land surface temperatures and increased SHF, coupled with a reduction in soil moisture and LHF, yield arid conditions. Such conditions can jeopardize the sustainability of the residual forested regions as well as agricultural activities in previously deforested areas (Dickinson and Henderson-Sellers 1988). Furthermore, tropical deforestation sets in motion a feedback loop: it fosters the propagation of drought conditions and, when combined with elevated temperatures and heightened water stress, further exacerbates the mortality rates of trees. This cycle of deterioration ultimately perpetuates the adverse effects of deforestation.

v. On a short-term (biophysical) timescale deforestation type LULC change influences both the weather and climate by altering the land-surface energy fluxes. While the conclusions drawn from proxy tropical deforestation design experiments using RCM (RegCMv4.4.5.10) are open for further exploration, possibly using a non-hydrostatic version of the ICTP-RegCM coupled with an earth system model, the research conducted in this study provides simulations of the impact of various deforestation scenarios on the Indian monsoon hydro-climate. These insights can be used to inform policy and management decisions related to land use, conservation, and climate change adaptation in the region.

vi. The findings of the study add significant value to the existing knowledge on the impact of anthropogenic activities, particularly deforestation on climate change and monsoon variability. It specifically highlights how the deforestation induced feedback influences the interannual variability of ISM precipitation and surface fluxes. It has profound implications for diverse socioeconomic sectors from agriculture to human health in India and other LMICs where adaptation and mitigation capacities are constrained due to inequity, high rates of informality, high debt service ratios, and high costs of capital among others. The paper's experimental design describes how deforestation contributes to alterations in albedo, roughness length, wind patterns, water evaporation and surface hydrological properties. It also details how these changes can impact regional climate patterns, leading to unpredictable temperature variability and humidity fluctuations. Such climate disruptions also bear financial implications for countries like India already dealing with many economic and infrastructure challenges.

vii. From an agro-economic perspective, the evidence provided by the study underscores the direct ramifications of variable monsoon patterns on food security and agricultural sustainability. For instance, the standard deviation of rainfall as seen in Fig. 17(a and b) shows relatively small variability over north-western India during the months of May to July in the scenario of deforestation potentially disrupting agricultural productivity (also monsoon precipitation decreases). This threatens the livelihoods of a large proportion of the population reliant on agriculture, potentially leading to forced migration and other socio-economic disruptions. From a policy perspective, these findings highlight the urgent need for effective adaptation and mitigation strategies as recognized in the recent COP 27 summit. Sustainable land-use planning, afforestation, and reforestation efforts should be a priority to alleviate the impacts of deforestation on monsoon patterns and related socioeconomic consequences. In this regards, land–atmosphere interactions using Dirmeyer's indices for various landuse—land cover change like afforestation, desertification, irrigation intensification is also planned as a future work.

viii. The study also underscores the differential impacts of these environmental changes on various social groups. The vulnerable and marginalized resource-dependent communities, particularly those with limited access to information are at high risk from climate change. It aligns with the IPCC Sixth Assessment Report, that emphasizes on socially just and equitable climate resilient development pathways, indicating a need for more inclusive, meaningful, and comprehensive communication and action strategies. The study thus provides a holistic perspective of tropical deforestation on climate of India, connecting climate research and need for climate adaptation.

Supplementary Information The online version contains supplementary material available at https://doi.org/10.1007/s11069-024-06615-z.

Acknowledgements International Centre for Theoretical Physics, Trieste, Italy is acknowledged for making the RegCMv4.4.5.10 model codes available for this study. The RegCMv4.4.5.10 executables were built on central HPC computing facilities available at Computer Services Centre and Centre for Atmospheric Sciences, IIT Delhi. National Center for Environmental Prediction/National Center for Atmospheric Research acknowledged for providing high-resolution meteorological datasets for setting the initial and boundary conditions to run the model. NCAR and UCAR are acknowledged for NCL and NETCDF4, analysis and software packages, respectively. The Grid Analysis and Display System (GrADS) version 2.0 software, NCAR Command Language (Version 6.2.0), Ultra scale Visualization Climate Data Analysis Tools (UVCDAT) package built with Python 2.7.4 and SciPy package (http://www.scipy.org/), are used for scientific computation and plotting. Wealth of online resource available at scholar.google.com was also helpful. The first

author is grateful towards MHRD, Govt. of India, Institute student fellowship supporting his Ph.D. research work. The authors also acknowledge Lund University, Sweden for providing research support. With deepest respect the first author offers gratitude towards faculty members at CAS, IIT Delhi: Prof. H. C. Upadhyaya, Prof. A. D. Rao and Prof. Somnath B. Roy for providing time to time advice. Finally, Johan Eckdahl (Ph.D.) and Gautam Sharma (Ph.D.) are thanked for helping in the final editing of the manuscript.

Author contributions The author Dr. Abhishek Lodh conceptualized and designed the study, developed the methodology, installed and run the regional climate model, curated the data, developed the verification and other scripts along with software, visualized the results, wrote the first draft of the paper, reviewed and edited the final document. The second author, Dr. Stuti Haldar, reviewed and edited the manuscript in current context of regional climate change and provided insights into the socioeconomic implications of the study. Both the authors discussed the results and commented on the manuscript's findings.

Funding Open access funding provided by Lund University.

Data availability The datasets generated from RegCMv4.4.5.10 model run and/or analyzed during the current study are available from the corresponding author on reasonable request.

Declarations

Conflict of interest The authors declare that they have no known competing financial interests or personal relationships that could have appeared to influence the work reported in this paper.

References

BaidyaRoy S, Avissar R (2002) Impact of land use/land cover change on regional hydrometeorology in Amazonia. J Geophys Res 107(D20):8037. https://doi.org/10.1029/2000JD000266

Bathiany S, Claussen M, Brovkin V, Raddatz T, Gayler V (2010) Combined biogeophysical and biogeochemical effects of large-scale forest cover changes in the MPI earth system model. Biogeosciences 7:1383–1399. https://doi.org/10.5194/bg-7-1383-2010

Bhowmick M, Parker DJ (2018) Analytical solution to a thermodynamic model for the sensitivity of afternoon deep convective initiation to the surface Bowen ratio. Q J R Meteorol Soc 144:2216–2229. https://doi.org/10.1002/qj.3340

Bollasina M, Nigam S (2011) Modeling of regional hydroclimate change over the indian subcontinent: impact of the expanding thar desert. J Clim 24:3089–3106. https://doi.org/10.1175/2010JCLI3851.1

Boysen LR, Brovkin V, Pongratz J, Lawrence DM, Lawrence P, Vuichard N, Peylin P, Liddicoat S, Hajima T, Zhang Y, Rocher M, Delire C, Séférian R, Arora VK, Nieradzik L, Anthoni P, Thiery W, Laguë MM, Lawrence D, Lo MH (2020) Global climate response to idealized deforestation in CMIP6 models. Biogeosciences 17:5615–5638. https://doi.org/10.5194/bg-17-5615-2020

Bretherton CS, McCaa JR, Grenier H (2004) A new parameterization for shallow cumulus convection and its application to marine subtropical cloud-topped boundary layers. Part I: description and 1D results. Mon Wea Rev 132:864–882. https://doi.org/10.1175/1520-0493(2004)132%3c0864:ANPFSC%3e2.0.CO;2

Camara M, Diba I, Diedhiou A (2022) Effects of land cover changes on compound extremes over west Africa using the regional climate model regCM4. Atmosphere 13:421. https://doi.org/10.3390/atmos13030421

Chambwera M, Heal G, Dubeux C, Hallegatte S, Leclerc L, Markandya A, McCarl BA, Mechler R, Neumann JE (2014) Economics of adaptation. In: Field CB, Barros VR, Dokken DJ, Mach KJ, Mastrandrea

MD, Bilir TE, Chatterjee M, Ebi KL, Estrada YO, Genova RC, Girma B, Kissel ES, Levy AN, MacCracken S, Mastrandrea PR, White LL (eds) Climate change 2014: impacts, adaptation, and vulnerability. Part A: global and sectoral aspects. Contribution of working group II to the fifth assessment report of the intergovernmental panel on climate change. Cambridge University Press, Cambridge, pp 945–977

Charney JG (1975) Dynamics of deserts and drought in the Sahel. Q J R Meteorol Soc 101:193–202. https://doi.org/10.1002/qj.49710142802

Charney J, Stone PH, Quirk WJ (1975) Drought in the sahara: a biogeophysical feedback mechanism. Science 187:434–435. https://doi.org/10.1126/science.187.4175.434

Charney J, Quirk WJ, Chow S-H, Kornfield J (1977) A comparative study of the effects of albedo change on drought in semi-arid regions. J Atmos Sci 34:1366–1385. https://doi.org/10.1175/1520-0469(1977)034%3c1366:ACSOTE%3e2.0.CO;2

Clement V, Rigaud KK, de Sherbinin A, Jones B, Adamo S, Schewe J, Sadiq N, Shabahat E (2021) Groundswell part 2: acting on internal climate migration. World Bank, Washington, DC

Dash SK, Pattnayak KC, Panda SK, Vaddi D, Mamgain A (2015) Impact of domain size on the simulation of Indian summer monsoon in RegCM4 using mixed convection scheme and driven by HadGEM2. Clim Dyn 44:961–975. https://doi.org/10.1007/s00382-014-2420-1

Devaraju N, Bala G, Modak A (2015) Effects of large-scale deforestation on precipitation in the monsoon regions: remote versus local effects. Proc Natl Acad Sci. https://doi.org/10.1073/pnas.1423439112

Dickinson RE (1983) Land surface processes and climate surface albedos and energy-balance. Adv Geophys 25:305–353. https://doi.org/10.1016/S0065-2687(08)60176-4

Dickinson RE, Henderson-Sellers A (1988) Modeling tropical deforestation—a study of GCM land surface parametrizations. Q J R Meteor Soc 114:439–462. https://doi.org/10.1002/qj.49711448009

Dickinson RE, Errico RM, Giorgi F, Bates GT (1989) A regional climate model for the western United States. Clim Change 15:383–422. https://doi.org/10.1007/BF00240465

Dickinson RE, Henderson-Sellers A, Kennedy PJ, Wilson MF (1986) Biosphere-atmosphere transfer scheme (BATS) for the NCAR COMMUNITY climate model (No. NCAR/TN-275-+STR). University corporation for atmospheric research. https://doi.org/10.5065/D6668B58

Dickinson RE, Henderson-Sellers A, Kennedy PJ (1993) Biosphere-atmosphere transfer scheme (BATS) Version 1e as coupled to the NCAR community climate model (No. NCAR/TN-387+STR). University corporation for atmospheric research. https://doi.org/10.5065/D67W6959

Dirmeyer PA, Shukla J (1994) Albedo as a modulator of climate response to tropical deforestation. J Geophys Res 99(D10):20863–20877. https://doi.org/10.1029/94JD01311

Durieux L, Machado LAT, Laurent H (2003) The impact of deforestation on cloud cover over the Amazon arc of deforestation. Remote Sens Environ 86(1):132–140. https://doi.org/10.1016/S0034-4257(03)00095-6

Elguindi N, Bi X, Giorgi F, Nagarajan B, Pal J, Solmon F, Rauscher S, Zakey A, O'Brien T, Nogherotto R, Giuliani G (2014) Regional climate model RegCM4.4 user manual

Eltahir EAB (1996) The role of vegetation in sustaining large-scale atmospheric circulations in the tropics. J Geophys Res 101(D2):4255–4268. https://doi.org/10.1029/95JD03632

Farid M, Keen M, Papaioannou M, Parry I, Pattillo C, Ter-Martirosyan A, IMF Staff (2016) After Paris: fiscal, macroeconomic and financial implications of global climate change. International monetary fund. https://www.imf.org/external/pubs/ft/sdn/2016/sdn1601.pdf

Ferranti L, Slingo JM, Palmer TN, Hoskins BJ (1999) The effect of land-surface feedbacks on the monsoon circulation. Q J R Meteorol Soc 125:1527–1550. https://doi.org/10.1002/qj.49712555704

Giorgi F, Coppola E, Solmon F, Mariotti L, Sylla MB, Bi X, Elguindi N, Diro GT, Nair V, Giuliani G, Turuncoglu UU, Cozzini S, Güttler I, O'Brien TA, Tawfik AB, Shalaby A, Zakey AS, Steiner AL, Stordal F, Sloan LC, Brankovic C (2012) RegCM4: model description and preliminary tests over multiple CORDEX domains. Clim Res 52:7–29. https://doi.org/10.3354/cr01018

Giorgi F, Elguindi N, Cozzini S, Solmon F, Giuliani G (2015) Regional climatic model RegCM user's guide version 4.4. Technical report. ICTP, Trieste, Italy

Gupta A, Thapliyal PK, Pal PK, Joshi PC (2005) Impact of deforestation on Indian monsoon: A GCM sensitivity study. J Indian Geophys Union 9(2):97–104

Harris NL, Gibbs DA, Baccini A, Birdsey RA, de Bruin S, Farina M, Fatoyinbo L, Hansen MC, Herold M, Houghton RA, Potapov PV, Requena SD, Roman-Cuesta RM, Saatchi SS, Slay CM, Turubanova SA, Tyukavina A (2021) Global maps of twenty-first century forest carbon fluxes. Nat Clim Change 11:234–240. https://doi.org/10.1038/s41558-020-00976-6

Hasler N, Werth D, Avissar R (2009) Effects of tropical deforestation on global hydroclimate: a multimodel ensemble analysis. J Clim 22:1124–1141. https://doi.org/10.1175/2008JCLI2157.1

Henderson-Sellers A, Dickinson RE, Durbidge TB, Kennedy PJ, McGuffie K, Pitman AJ (1993) Tropical deforestation—modeling local-scale to regional-scale climate change. J Geophys Res Atmos 98:7289–7315. https://doi.org/10.1029/92JD02830

Holtslag AAM, Boville BA (1993) Local versus nonlocal boundary-layer diffusion in a global climate model. J Climate 6:1825–1842. https://doi.org/10.1175/1520-0442(1993)006%3c1825:LVNBLD%3e2.0.CO;2

Holtslag AAM, De Bruijn EIF, Pan H (1990) A high-resolution air mass transformation model for short-range weather forecasting. Mon Weather Rev 118:1561–1575. https://doi.org/10.1175/1520-0493(1990)118%3c1561:AHRAMT%3e2.0.CO;2

Kanamitsu M, Ebisuzaki W, Woollen J, Yang S, Hnilo JJ, Fiorino M, Potter GL (2002) NCEP–DOE AMIP-II reanalysis (R-2). Bull Am Meteor Soc 83(11):1631–1644. https://doi.org/10.1175/BAMS-83-11-1631

Kim D-H, Sexton JO, Townshend JR (2015) Accelerated deforestation in the humid tropics from the 1990s to the 2000s. Geophys Res Lett 42:3495–3501. https://doi.org/10.1002/2014GL062777

Kovats RS, Hajat S (2008) Heat stress and public health: a critical review. Annu Rev Public Health 29:41–55. https://doi.org/10.1146/annurev.publhealth.29.020907.090843

Krishnamurti TN, Bhalme HN (1976) Oscillations of a monsoon system. Part I observational aspects. J Atmos Sci 33:1937–1954. https://doi.org/10.1175/1520-0469(1976)033%3c1937:OOAMSP%3e2.0.CO;2

Lawrence D, Vandecar K (2015) Effects of tropical deforestation on climate and agriculture. Nature Clim Change 5:27–36. https://doi.org/10.1038/nclimate2430

Leite-Filho AT, Soares-Filho BS, Davis JL, Abrahão GM, Börner J (2021) Deforestation reduces rainfall and agricultural revenues in the Brazilian amazon. Nat Commun 12:2591. https://doi.org/10.1038/s41467-021-22840-7

Li Y, Zhao M, Mildrexler DJ, Motesharrei S, Mu Q, Kalnay E, Zhao F, Li S, Wang K (2016) Potential and actual impacts of deforestation and afforestation on land surface temperature. J Geophys Res Atmos 121:14372–14386. https://doi.org/10.1002/2016JD024969

Lodh A (2017) Simulated impact of desertification and deforestation on Indian monsoon rainfall and surface fluxes. J Ecosyst Ecogr 7:226. https://doi.org/10.4172/2157-7625.1000226

Lodh A (2020) Reassessment of land–atmosphere interactions over India during summer monsoon using state-of-the-art regional climate models. Theor Appl Climatol 142:1649–1673. https://doi.org/10.1007/s00704-020-03395-x

Lodh A (2021) Simulating the impact of extended desertification on Indian hydro climate using ICTP-RegCM4.4.5.10 model. J Hydrol 598:126405. https://doi.org/10.1016/j.jhydrol.2021.126405

Lorenz R, Pitman AJ, Sisson SA (2016) Does Amazonian deforestation cause global effects; can we be sure? J Geophys Res Atmos 121:5567–5584. https://doi.org/10.1002/2015JD024357

Mabuchi K (2011) A numerical investigation of changes in energy and carbon cycle balances under vegetation transition due to deforestation in the Asian tropical region. J Meteorol Soc Jpn 89(1):47–65. https://doi.org/10.2151/jmsj.2011-104

Mabuchi K, Sato Y, Kida H (2005) Climatic impact of vegetation change in the Asian tropical region. Part I: case of the northern hemisphere summer. J Clim 18:410–428. https://doi.org/10.1175/JCLI-3273.1

Marambe B, Punyawardena R, Silva P, Premalal S, Rathnabharathie V, Kekulandala B, Nidumolu U, Howden M (2015) Climate climate risk and food security in Sri Lanka: the need for strengthening adaptation strategies. In: Leal Filho W (ed) Handbook of climate change adaptation. Springer, Berlin, pp 1759–1789

New M, Reckien D, Viner D, Adler C, Cheong S-M, Conde C, Constable A, Coughlan de Perez E, Lammel A, Mechler R, Orlove B, Solecki W (2022) Decision-Making Options for Managing Risk. In: Climate Change (2022) Impacts, adaptation and vulnerability. Contribution of Working Group II to the Sixth Assessment Report of the Intergovernmental Panel on Climate Change, Cambridge University Press, Cambridge, UK and New York, NY, USA, pp 2539–2654. https://doi.org/10.1017/9781009325844.026

Pielke R, Avissar R, Raupach M, Dolman A, Zeng X, Denning A (1998) Interactions between the atmosphere and terrestrial ecosystems: influence on weather and climate. Glob Change Biol 4:461–475. https://doi.org/10.1046/j.1365-2486.1998.t01-1-00176.x

Polcher J, Laval K (1994a) The impact of African and Amazonian deforestation on tropical climate. J Hydrol 155(3):389–405. https://doi.org/10.1016/0022-1694(94)90179-1

Polcher J, Laval K (1994b) A statistical study of the regional impact of deforestation on climate in the LMD GCM. Clim Dyn 10(4–5):205–219. https://doi.org/10.1007/BF00208988

Pörtner H-O, Roberts DC, Adams H, Adelekan I, Adler C, Adrian R, Aldunce P, Ali E, Bednar-Friedl B, Begum RA, Bezner Kerr R, Biesbroek R, Birkmann J, Bowen K, Caretta MA, Carnicer J, Castellanos E, Cheong TS, Chow W, Cissé G, Clayton S, Constable A, Cooley SR, Costello MJ, Craig M, Cramer W, Dawson R, Dodman D, Efitre J, Garschagen M, Gilmore EA, Glavovic BC, Gutzler D, Haasnoot M, Harper S,

Hasegawa T, Hayward B, Hicke JA, Hirabayashi Y, Huang C, Kalaba K, Kiessling W, Kitoh A, Lasco R, Lawrence J, Lemos MF, Lempert R, Lennard C, Ley D, Lissner T, Liu Q, Liwenga E, Lluch-Cota S, Löschke S, Lucatello S, Luo Y, Mackey B, Mintenbeck K, Mirzabaev A, Möller V, Moncassim Vale M, Morecroft MD, Mortsch L, Mukherji A, Mustonen T, Mycoo M, Nalau J, New M, Okem A, Ometto JP, O'Neill B, Pandey R, Parmesan C, Pelling M, Pinho PF, Pinnegar J, Poloczanska ES, Prakash A, Preston B, Racault M-F, Reckien D, Revi A, Rose SK, Schipper ELF, Schmidt DN, Schoeman D, Shaw R, Simpson NP, Singh C, Solecki W, Stringer L, Totin E, Trisos CH, Trisurat Y, van Aalst M, Viner D, Wairiu M, Warren R, Wester P, Wrathall D, Zaiton Ibrahim Z (2022) Climate change 2022: Impacts, adaptation, and vulnerability. Contribution of working group II to the sixth assessment report of the intergovernmental panel on climate change. Cambridge University Press, pp 37–118

Rasul G, Sharma B (2016) The nexus approach to water–energy–food security: an option for adaptation to climate change. Climate Policy 16(6):682–702. https://doi.org/10.1080/14693062.2015.1029865

Revi A, Roberts D, Klaus I, Bazaz A, Krishnaswamy J, Singh C, Eichel A, Kodira PP, Seth S, Adelekan I, Babiker M, Bertoldi P, Cartwright A, Chow W, Colenbrander S, Creutzig F, Dawson R, De Coninck H, De Kleijne K, Dhakal S, Gallardo L, Garschagen M, Haasnoot M, Haldar, S, Hamdi R, Hashizume M, Islam AKMS, Jiang K, Kılkış S, Klimont Z, Lemos MF, Ley D, Lwasa S, McPhearson T, Niamir L, Otto F, Pathak M, Pelling M, Pinto I, Pörtner H-O, Pereira JP, Raghavan K, Roy J, Sara LM, Seto KC, Simpson NP, Solecki W, Some S, Sörensson AA, Steg L, Szopa S, Thomas A, Trisos C, Urge-Vorsatz D (2022) The Summary for Urban Policymakers of the IPCC's Sixth Assessment Report. Indian Institute for Human Settlements. https://doi.org/10.24943/SUPSV511.2022

Reynolds RW, Rayner NA, Smith TM, Stokes DC, Wang W (2002) An improved in-situ and satellite SST analysis for climate. J Clim 15:1609–1625. https://doi.org/10.1175/1520-0442(2002)015%3c1609:AIISAS%3e2.0.CO;2

Ripley EA (1976) Drought in the sahara: insufficient biogeophysical feedback? Science 191(4222):100–103. https://doi.org/10.1126/science.191.4222.100.a

Scharn R, Little CJ, Bacon CD, Alatalo JM, Antonelli A, Björkman MP, Molau U, Nilsson RH, Björk RG (2021) Decreased soil moisture due to warming drives phylogenetic diversity and community transitions in the tundra. Environ Res Lett. https://doi.org/10.1088/1748-9326/abfe8a

Sen OL, Wang Y, Wang B (2004) Impact of Indochina deforestation on the East Asian summer monsoon. J Clim 17:1366–1380. https://doi.org/10.1175/1520-0442(2004)017%3c1366:IOIDOT%3e2.0.CO;2

Shukla J, Mintz Y (1982) Influence of land-surface evapotranspiration on the earth's climate. Science 215(4539):1498–1501. https://doi.org/10.1126/science.215.4539.1498

Spracklen DV, Garcia-Carreras L (2015) The impact of Amazonian deforestation on Amazon basin rainfall. Geophys Res Lett 42:9546–9552. https://doi.org/10.1002/2015GL066063

Srinivasan M, Ghoge K, Haldar S, Bazaz A, Revi A (2023) Climate finance in India 2023. Indian Institute for Human Settlements. https://doi.org/10.24943/CFI11.2023

Stocker TF, Qin D, Plattner G-K, Tignor M, Allen SK, Boschung J, Nauels A, Xia Y, Bex V, Midgley PM (2013) IPCC, 2013: climate change 2013: the physical science basis. Contribution of working group I to the fifth assessment report of the intergovernmental panel on climate change. Cambridge University Press.

Strandberg G, Chen J, Fyfe R, Kjellström E, Lindström J, Poska A, Zhang Q, Gaillard M-J (2023) Did the bronze age deforestation of Europe affect its climate? A regional climate model study using pollen-based land cover reconstructions. Clim past 19:1507–1530. https://doi.org/10.5194/cp-19-1507-2023

Sud YC, Shukla J, Mintz Y (1988) Influence of land surface roughness on atmospheric circulation and precipitation: a sensitivity study with a general circulation model. J Appl Meteorol 27(9):1036–1054

Sud YC, Lau WK-M, Walker GK, Kim J-H, Liston GE, Sellers PJ (1996) Biogeophysical consequences of a tropical deforestation scenario: a GCM simulation study. J Clim 9(12):3225–3247. https://doi.org/10.1175/1520-0442(1996)009%3c3225:BCOATD%3e2.0.CO;2

Sundqvist H, Berge E, Kristjánsson JE (1989) Condensation and cloud parameterization studies with a mesoscale numerical weather prediction model. Mon Weather Rev 117:1641–1657. https://doi.org/10.1175/1520-0493(1989)117%3c1641:CACPSW%3e2.0.CO;2

Watson RT, Zinyowera MC, Moss RH (1997) The regional impacts of climate change: an assessment of vulnerability. Cambridge University Press, UK, p 517

Werth D, Avissar R (2002) The local and global effects of amazon deforestation. J Geophys Res 107(D20):8087

Werth D, Avissar R (2005a) The local and global effects of African deforestation. Geophys Res Lett 32:L12704. https://doi.org/10.1029/2005GL022969

Werth D, Avissar R (2005b) The local and global effects of Southeast Asian deforestation. Geophys Res Lett 32:L20702. https://doi.org/10.1029/2005GL022970

Xue Y, Shukla J (1993) The Influence of land surface properties on sahel climate Part I: Desertification. J Clim 6(12):2232–2245

Yasuoka J, Levins R (2007) Impact of deforestation and agricultural development on anopheline ecology and malaria epidemiology. Am J Trop Med Hyg 76:450–460

Yuan K, Zhu Q, Zheng S, Zhao L, Chen M, Riley WJ, Cai X, Ma H, Li F, Wu H, Chen L (2021) Deforestation reshapes land-surface energy-flux partitioning. Environ Res Lett. https://doi.org/10.1088/1748-9326/abd8f9

Zeng N, Neelin JD (1999) A land-atmosphere interaction theory for the tropical deforestation problem. J Clim 12:857–872. https://doi.org/10.1175/1520-0442(1999)012%3c0857:ALAITF%3e2.0.CO;2

Zheng X, Eltahir EAB (1997) The response to deforestation and desertification in a model of West African monsoons. Geophys Res Lett 24(2):155–158. https://doi.org/10.1029/96GL03925

Zickfeld K, Knopf B, Petoukhov V, Schellnhuber HJ (2005) Is the Indian summer monsoon stable against global change? Geophys Res Lett 32:L15707. https://doi.org/10.1029/2005GL022771

Authors and Affiliations

Abhishek Lodh[1,2,3] · Stuti Haldar[4,5]

✉ Abhishek Lodh
abhishek.lodh@nateko.lu.se; abhishek.iitd.lodh@gmail.com

[1] Department of Physical Geography and Ecosystem Science, Lund University, Sölvegatan 12, Lund 223 62, Sweden

[2] Swedish Meteorological and Hydrological Institute, Folkborgsvägen 17, Norrköping 601 76, Sweden

[3] Centre for Atmospheric Sciences, Indian Institute of Technology Delhi, Hauz Khas, New Delhi 110016, India

[4] Indian Institute for Human Settlements, Bangalore 560080, India

[5] Department of Design Sciences and CIRCLE - Centre for Innovation Research, Lund University, Sölvegatan 16, Lund 223 62, Sweden